Title
FOAM FRACTIOKATION OF RARE-EARTH ELEMENTS

Authors
Robertson, George H.
Vermeulen, Theodore.

Publication Date
1969-12-01

UCRL-19525

c. 2

FOAM FRACTIONATION OF RARE-EARTH ELEMENTS

George H. Robertson* and Theodore Vermeulen

December 1969

AEC Contract No. W-7405-eng-48

*Filed as a Ph. D. Thesis

LAWRENCE RADIATION LABORATORY
UNIVERSITY of CALIFORNIA BERKELEY

UCRL-19525

DISCLAIMER

FOAM FRACTIONATION OF RARE-EARTH ELEMENTS

Contents

FOAM FRACTIONATION OF RARE-EARTH ELEMENTS

George H. Robertson and Theodore Vermeulen

Department of Chemical Engineering and
Lawrence Radiation Laboratory
University of California
Berkeley, California

December 31, 1969

ABSTRACT

The foam fractionation of rare-earth elements Nd, Sm, and Ce by extraction of their EDTA chelates with a cationic surfactant, and the foam fractionation of an anionic surfactant were studied. The objective was to determine the usefulness of the foaming technique in fine separations and to examine quantitatively the properties of transient foaming in producing the separation.

The model of "persistent" foaming did not apply to most of the foaming conditions which were found in this study to favor foam formation, extraction, and fractionation. Therefore, a two-property classification was adopted; the type being determined by the persistence or transience of surface area, and the mode by the constancy or depletion of specific liquid content with foam height or age.

In a preliminary study, fixed-height foaming from aqueous solutions of an anionic surfactant (Aerosol 22) was

used to evaluate the effect of gas rate on the relative transiency and separation performance. Foaming of Aerosol-22 in a transient regime of gas rates yielded the best enrichments and extraction. The foam liquid fraction was proportional to the 0.20 power of the gas velocity in the transient regime and to the 0.71 power in the persistent regime.

No previous foam fractionation between rare-earth elements has been reported. For rare-earth separation, separate cationic surfactant (Hyamine 1622) and chelating agent (EDTA) were employed to obtain good foaming and extraction as well as selectivity. Experimental studies were made of solution variables (surfactant concentration, EDTA concentration, total rare-earth concentration) and of physical variables (foam height and column packings) on the relative foam stability, total rare-earth enrichment, separation factor, extraction rate, and foam liquid content.

Transient foaming for rare-earth separations was observed for all concentrations of surfactant tested; transiency increased as the surfactant concentration decreased. Enrichments of rare earth were best for the most transient foaming (lowest surfactant concentration). Separation factor (1.9 for Nd/Ce and 3.1 for Sm/Ce) was invariant above 17cm and decreased sharply to 1.0 below 17cm. Extraction, constant above 17cm, was best in the most transient foams.

Appreciable separation improvement was achieved by blocking foam with stacks of screens or plastic bead packings. These devices also increased the foam liquid content.

TABLES

FIGURES

INTRODUCTION

Adsorptive-Bubble Separation Methods

The objective of this thesis is to apply foam fractionation to the extraction and separation of rare-earth ions at low concentrations. Foam fractionation, one of the adsorptive-bubble separation methods (ABSM), uses gas bubbles to extract soluble chemical species from solution. The soluble species are extracted either because they are surface-active and adsorb on the bubble surfaces, or because they are attracted by charge interaction or chelate formation to a species which is surface-active.

Nearly all of the previous study of foaming utilizes stable foams. These foams may be characterized by bubble-size and liquid-density values that are independent of foam height. All of the semiquantitative design methods apply strictly only to foaming of stable or persistent foams. When unstable or transient foams have been encountered as they must be in batch exhaustive extractions, no quantitative description of the foam structure or of important design considerations has yet been given. Nevertheless, the mode of foaming (transient or persistent) may be extremely important to the effectiveness of the separation.

This work applies transient foaming to the extraction of an anionic surfactant and to the extraction/separation of

binary rare-earth solutions. The study is largely experimental. It adopts a method of classifying foaming, and demonstrates significant design implications of this classification.

Foam Fractionation

A process wherein particulate matter or a solution species is brought from a bulk area of a homogeneous solution or suspension to a surface area by attachment to a bubble can broadly be classified as an adsorptive-bubble separation method (K1). Although superficially similar in producing a foam or scum, the various types of ABSM possess quite different mechanisms to produce the subsequent separation. Table I below lists the various types of ABSM.

Foam fractionation, as a member of the adsorptive-bubble separation methods, is a process wherein only soluble solution species are drawn to the surface of a gas bubble and collected in a foam (L2). It differs from the other foaming ABSM in producing a true foam rather than a scum. Foam fractionation has been applied to the removal or concentration of surface-active species and to the removal or concentration of surface-inactive species by coadsorption.

Several important features of foam fractionation as an extraction technique should be pointed out. In the sense that the interactions between surfactant and counterion are on a mole-to-mole or electro-equivalent basis, the

Table I. Adsorptive-bubble separation methods**

A. Foaming Separations	
1. Foam fractionation	Removal of dissolved material by foaming.
2. Flotation	Removal of particulate material by foaming.
a. ore flotation	Particulate material is inorganic mineral.
b. ion flotation (ionic precipitate)*	Particulate material is product from surfactant and nonsurfactive ionic species.
c. molecular flotation (molecular precipitate)*	Like (b) but with nonsurfactive nonionic species.
d. precipitate flotation (activated precipitate)*	Particulate material is a precipitate; the precipitating agent is nonsurfactive.
e. adsorbing-colloid flotation	Removal of material by adsorption on colloidal particles, followed by flotation of these particles.
B. Nonfoaming Separations	
1. Bubble fractionation	Removal of material (molecular or particulate) by virtue of adsorption at the surface of rising bubbles.
2. Solvent sublation	Removal of material (molecular or particulate) by virtue of adsorption at the surface of rising bubbles followed by deposition within, or at the horizontal interface of an immiscible liquid atop the main liquid.

* Names suggested to be more in accord with the mechanism by which process occurs.

** This listing is different from recently published listings (K1,L2) in eliminating categories based on the size of the extracted species: macro-flotation and micro-flotation.

process is stoichiometric, but because of contamination of the foam with bulk entrained fluid, the end result of a foaming may not appear to be stoichiometric. Competition exists between surface and micellar formations for the metal species which is to be extracted. Competition exists between complexed and uncomplexed species for surface positions. The pH can control enrichment because of competition between H^+ and positive metallic ions, and because of its effect on the ionization of the surfactant if ionizable. Operating conditions affect the absolute enrichment in a foam. The surfactant action in extraction is through charged-monolayer interaction or complex formation. The separations achievable depend upon the ionic strength of the solution.

Ion Flotation

Of the other adsorptive-bubble separations, ion flotation is most often confused with foam fractionation, and will sometimes occur simultaneously. In an ion flotation, the surfactant-ion combination is insoluble, and the product is collected as a scum rather than a foam. This insolubility effect involves a change in the mechanism of attraction at the bubble surface; since the insoluble product is no longer heteropolar, flotation occurs because of hydrophobicity of the particle surface and buoyancy of the particle-bubble combination. The presence of a scum

necessitates the operation of the extraction device at low gas flow rates to prevent redispersion of particles collected at the surface.

Ion flotation, moreover, is a rate process in which the concentration of sublate (surfactant-ion combination) reaches equilibrium in an initial area of gas-liquid interface, and then apparently supersaturates as physical coalescence reduces the available interfacial area. When the increasing concentration exceeds the solubility limit, the sublate crystallizes and appears as a scum. This is a local effect and occurs adjacent to solution whose total concentration still lies below the solubility limit for the ion-surfactant combination. Sebba (S6) has discussed this at some length.

Whether or not a given system operates as a foam fractionation, an ion flotation, or a precipitate flotation depends on the chain length of the surfactant, the pH, the ionic strength, the concentration and solubility of the collector-colligend combination in the solution and at the interface, and the chemical nature of the colligend under the conditions of the separation. As one proceeds from initially soluble to initially insoluble or colloidal systems, the resultant foam behavior (as classified in Table I) ranges from foam fractionation to precipitate flotation, and the surfactant requirements decrease from stoichiometric amounts to less than stoichiometric amounts.

Comparison studies of variables on a limited number of systems have been made by Rubin, Johnson, and Lamb (R4), Rubin (R1), and Grieves, Bhattacharyya, and Conger (G2).

An additional difference between ion flotation and foam fractionation may be observed in the nature of the specific interactions. In an ion flotation, the specificity between ionic constituents is independent of the interface composition, and depends only on relative activities and free energies of formation in the bulk solution. This specificity is only observed at the interface where precipitation occurs. In foam fractionation, the specificity depends on charge interaction and complex formation that occur at the interface between the gas bubble and the solution, and will differ from the selectivity obtained in noninterfacial processes with the same reagents. Although Table I implies strict classification, in many systems the mode of operation may be intermediate between two or more types.

The published research on ion flotation done by Sebba (S6,S7,S8,S9,S14) and Grieves (G4) has concentrated largely on extraction of individual ions or on separations in which one species was wholly complexed and one was uncomplexed. Little work has been done to investigate interionic separations, due perhaps to the difficulty in handling flow streams containing solids. This difficulty may be

compounded in cascaded systems, which are usually necessary for complete interionic separations.

Foam Stability

In order to separate any substance from its aqueous solution by foaming, either that substance or some other component in the solution must possess certain properties which enable it to form a foam. Kitchener (K4,K5) identified these to be film elasticity, fluid viscosity, and double-layer repulsion between adjacent bubble surfaces. These contributions in varying amounts will result in varying degrees of foam stability.

Film elasticity is the restoring force produced under the action of any stress that tends to extend the area of the film. The usual source of this elastic action is the depletion of an adsorbed surface layer. This force arises from local stretching that raises the surface tension by decreasing the average solute concentration in the film. This result, observed also in the Marangoni effect, applies particularly to thin films where the underlying liquid contains only a limited quantity of solute. This restoring force largely explains the dependence of foam stability upon concentration of foaming agent. Too dilute a solution means that the range of surface tension values which promote stability is severely limited. Too concentrated a solution means that diffusion of reserve material to the

surface will restore the initial surface tension too quickly for a restoring force to be active.

The enhanced viscosity of a foaming solution is important because it retards drainage of liquid from between individual bubbles. The action of viscosity in retarding coalescence can be seen in small-bubble dispersions in very viscous fluids, where foams may be formed in the absence of any surface-active substance.

The foamability of solutions has been measured in a number of ways (B4), such as persistence of single bubbles, persistence of vertical films, steady-state foam height, rate of foam decay, and rate of drainage out of the foam. These criteria are not especially useful in understanding the detailed history of foam formation and decay.

The classification of foams as stable or unstable (persistent or transient) is a relative matter, since no foam (unless solidified) can be maintained indefinitely. Furthermore, the visually observed results of foaming depend not only on the specific properties of the foaming agent, but equally on experimental conditions such as gas flow rate and column height.

For continuous operations, the stability or instability of the "foaming", i.e. of the formation and transport of foam, will be identified with the corresponding stability or instability that is produced by the combination of

compositional and physical factors used. A knowledge of the foam structure changes -- the loss of surface and the loss of intersticial liquid -- which characterize the stability of the foaming will be important to the optimum design of a foaming column.

Foaming Devices

A foaming device may operate as either a single-contact or a multiple-contact device. In a single-contact device, every gas bubble injected into the bottoms pool takes its place in the foam; it does not break or coalesce with any other foam bubble. It withdraws its complement of collector and colligend from the surrounding pool liquid. When it passes into the foam, a certain amount of pool liquid is withdrawn with it, so that the net effect is a somewhat smaller enrichment than could have been obtained by extracting only the liquid associated with the bubble surface. As a consequence of intersticial drainage of pool-like liquid, the enrichment may vary over wide limits.

A multiple-contact foam device is one in which coalescence and breakage readily occur at the top of, and within, the foam matrix. The result is that each rising bubble at or near the bottom of the matrix draws its complement of collector and colligend from the intersticial liquid, which is no longer pool-like but has been enriched by the collector and colligend extracted from the downflowing liquid initially

associated with the now-broken foam bubbles. Enrichments achieved in multiple-contact single-stage devices should be greater than in single-contact single-stage devices, but are also subject to wide variations associated with drainage effects. In practical cases, the coalescence desired for good multiple contacting may be induced by column geometries which distort or stress the foam.

The most common apparatus reported (L2) are shown schematically in Figure 1. All of these may operate as multiple-contact devices, depending on the nature of the foam exit and the nature of the foam itself. For a noncoalescing foam, only the refluxed columns will operate as multiple-contact, single-stage devices. Stripping columns have been used (L2) in application to very dilute process streams. In these applications the feed stream is added to the foam. This addition may be made at any level although provision is generally made for a drainage section above the midpoint.

The experimental apparatus used in foaming studies have usually been vertically mounted, constant diameter (up to 50 mm), and fixed height (up to 100 cm) glass columns (R3). Columns as large as 4 inches in diameter and 6 ft tall have been studied (S12). A decreasing-diameter foam-drainage section has been applied by Schutz (S15) to provide support for a coalescing foam. A horizontal foam-drainage section has been used to minimize entrainment caused by vertically rising foam bubbles (H2).

a. Batch operation

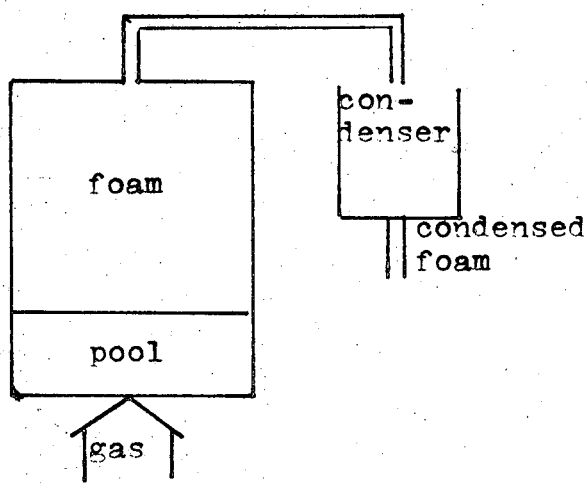

b. Continuous operation

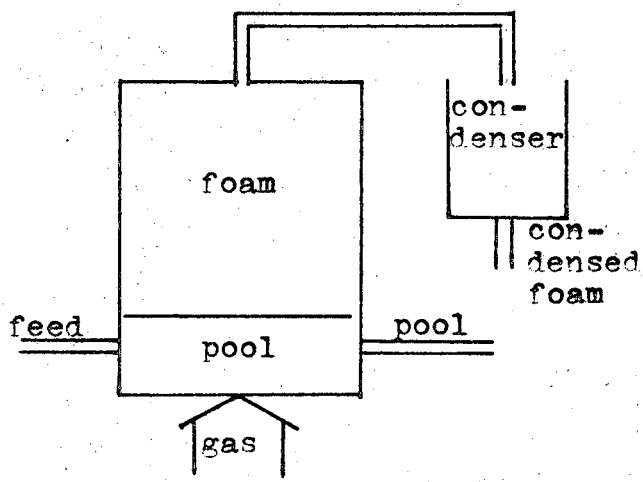

c. Batch with external recycle

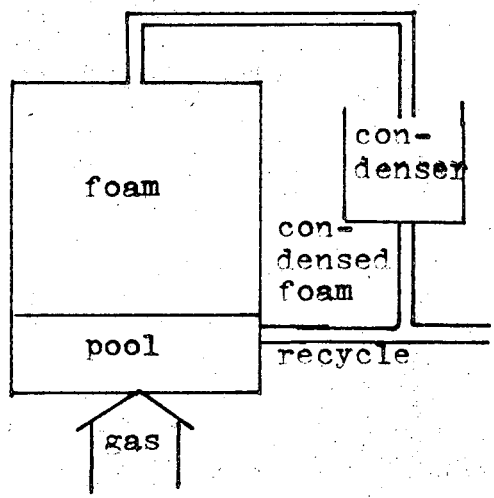

Figure 1. Schematic foam fractionation units (L2).

Gas sparging has been accomplished with stainless-steel spinerettes (S1), sintered-glass bubblers (B1, S12), and single orifices (R3). One obtains decreasing bubble-size uniformity using orifices, spinerettes, and bubblers.

Column cascades in which foam is condensed and refoamed in a second apparatus have been examined by Jacobelli-Turi et al. (J2) in the ion extraction of uranium complexes.

Countercurrent flow of foam and pool liquid in a staged apparatus was tested in foaming of dodecyl benzene sulfonate. The column was fitted with bubble-cap trays (as in a distillation) with downcomers external to the column. Tray efficiencies of 30% were reported (W2).

General Foam-Pool Relations

A material balance for any foam operating continuously with feed, condensed foam, and pool flowstreams as shown in Figure 2 will be

$$Fc_f = Pc_p + S_v c_s \qquad (1)$$

Here F, P, and S_v are the liquid volumetric rates of the feed, pool, and foam streams respectively, and c_f, c_p, and c_s are the concentrations of these streams.

The result of dividing the last term into portions to account for mass associated with the bulk liquid and surface in the foam is

$$Fc_f = Pc_p + Sf + S_b c_p \qquad (2)$$

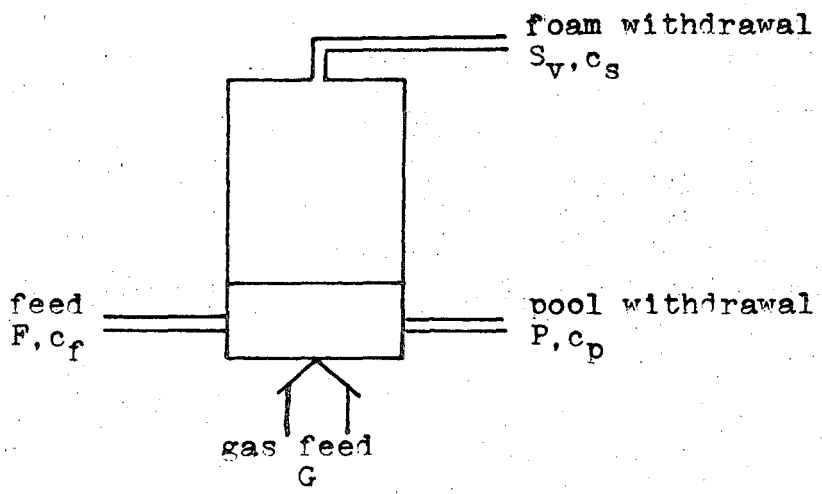

Figure 2. Continuous flow foam fractionation unit (L2).

where S is the area generation rate, Γ is the surface excess, and S_b is the bulk liquid rate for the foam. The area-generation rate can be replaced by $6G/d$, where G is the dry-gas flow rate and $6/d$ is the ratio of surface to volume for bubbles of size d. It is commonly assumed that $S_b = S_v$; that is, that the volume associated with the surface is negligible.

Substitution and rearrangement yield

$$\Gamma = (Fc_f - Pc_p - S_v c_p)/(6G/d) \tag{3}$$

or

$$\Gamma = (Fc_f - c_p(P + S_v))/(6G/d) \tag{4}$$

Dividing by c_p gives the distribution coefficient

$$\Gamma/c_p = (F(c_f/c_p) - (P + S_v))/(6G/d) \tag{5}$$

and accounting for the volumetric balance gives

$$\Gamma/c_p = (Fd/6G)(c_f/c_p - 1)$$

$$= (Fd/6G)(E - 1) \tag{6}$$

where E is the enrichment ratio for any species or group of species in solution.

An alternative to dividing the foam mass into surface and intersticial contributions, as in Equation 2, has been

provided by Grieves' empirical approach to the foaming process (G3), relating the composition of the entire foam mass to that of the bulk pool:

$$S_V c_S = mG(F)^{\frac{1}{3}} \tag{7}$$

where m is an empirical function of the feed concentration for any given surfactant.

The separation factor for the foaming process is defined by

$$\alpha = (c_{as}c_{bp})/(c_{bs}c_{ap}) \tag{8}$$

The effective mass extraction rate, M, may be defined as

$$M = (E - 1)c_p S_V \tag{9}$$

and this is equal to FS for high enrichments.

Semiquantitative predictions of expected enrichments may be made on the basis of several approximations. Assuming spherical bubbles and a specific area of 30 $Å^2$ for each surfactant molecule, the surface capacity is about 0.5×10^{-9} gm-moles/cm^2, and the volumetric capacity is obtained by multiplying the surface generation rate by 6G/d. Clearly, this calculation takes no account of the entrainment, but may be useful as an approximation when entrainment data are

not available. If the enrichment ratio is large, as in stripping operations, the knowledge of the entrainment is less important.

Multiple-Stage Operation. A calculational procedure has been suggested by Eldib (E1) for relating the number of cascaded equilibrium stages to the separation produced. The procedure used is analogous to McCabe-Thiele analysis of distillation, in which the operating line is given by a component material balance, and equilibrium is given by

$$c_s = c_p + AN_0F \tag{10}$$

Here N_0 is the molecular weight. A is the ratio of surface area to liquid foam volume and is a function of linear gas rate, bubble size, and foam residence time; it is evaluated by experiment, or by a predictive equation as discussed below in Foam Density.

The operating line for the enriching section is described by

$$(c_s)_{n+1} = c_pR/(R+1) + c_D/(R+1) \tag{11}$$

where n is a stage index, c_p refers to the concentration of surfactant in the bulk intersticial space, c_D refers to the condensed foam concentration, and R is the ratio of downflowing liquid to total withdrawn condensed foam--the reflux ratio.

In applying McCabe-Thiele analysis to the foaming unit, each ideal stage corresponds to a single-stage device, as long as the device operates on a single contact. If multiple contacts do occur, then each calculated ideal stage will correspond to a fraction of a single-stage device. If multiple contacts are allowed, however, the equations for both the equilibrium line and the operating line are no longer strictly correct. This is a consequence of the equilibrium curve being a function of bubble size and foam structure, both of which change in a multiple-contact device; and the slope of the operating line being no longer constant, since the reflux ratio will change drastically for a coalescing foam.

Lemlich (L2,L3) has considered a composite multistage cascade with both stripping and enriching sections.

Up to this point, the terms for adsorption density (Γ) and liquid content of the foam (A) have been left general. The sections immediately following describe exact and approximate methods for inter-relating these terms.

Equilibrium Adsorption Density

The result of the thermodynamic theory, the Gibbs adsorption isotherm (A1), relates the surface concentration to the gradient of surface free energy (surface tension) with chemical potential:

$$d\gamma = -\sum_{i=1}^{w} \Gamma_i d\mu_i \qquad (12)$$

where γ is the surface tension, μ_i is the chemical potential of species i, and Γ_i is the adsorption density in moles/cm^2. Various conventions are employed to increase the usefulness of this equation, as reviewed elsewhere (M4,R3). The simplest, the Gibbs convention, assigns $\Gamma = 0$ for the solvent. This is equivalent to computing the excess by comparing a surface layer containing n moles of solvent to a "layer" of bulk solution containing n moles of solvent. The excess of components 2,3,...n is given by

$$d\gamma = -\sum_{i=2}^{w} \Gamma_i d\mu_i \qquad (13)$$

It should be noted that Equation 14 below may be substituted for the chemical potential in Equation 13.

$$d\mu_i = RTd\ln a_i \qquad (14)$$

where a_i is the activity of species i and is equivalent to the product of concentration and activity coefficient. In many dilute solutions the activity coefficient is unity, and then concentrations may be substituted directly for activities.

Cases of adsorption of ionic and nonionic surfactants from solutions of differing ionic strengths have been considered by Moilliet et al. (M4).

Surface-adsorption predictions based on a rigorous thermodynamic analysis are extremely difficult in complex systems because of the number of species to be accounted; consequently most investigators are satisfied to make a few foaming experiments rather than extensive surface-tension measurements. Furthermore, the theory applies only to persistent foams and probably not to transient foams in which the surface area is always changing.

Surface-tension measurement of single-component solutions was not sufficient to predict the relative amounts of two surfactants, sodium lauryl sulfate and sodium dodecyl benzene sulfate, on the surfaces of foams formed from solutions containing both agents (J4).

Coadsorption of Nonsurfactive Species. Application of foaming to the extraction of nonsurfactive species requires a method of predicting the specificity of the foam surface for individual ions in the solution. This specificity may arise from charge interactions between the adsorbed surfactant layer and a diffuse-double-layer of counterions, or from bonded interactions of a chelate type between surfactant and solution species.

Competitive coadsorption of ions of opposite charge to the surfactant has been predicted by Jorné (J3), based on the diffuse-double-layer theory of Gouy and Chapman, and allowing for differences in the distance of closest approach of

ions of different size. The theory is best summarized by dividing it into consideration of like-sized but unlike-charged ions, and then extending it to different-sized ions.

(a) Like-sized ions. Assumptions made are that charges are point charges, curvature of the interface is negligible, and excess surfactant is concentrated at the interface in a monolayer. The excess of an individual ion i may then be defined as

$$\Gamma_i/n_{\infty i} = \int_{x=x_o}^{x=\infty} (v^{z_i} - 1)dx \qquad (15)$$

where $n_{\infty i}$ is the bulk concentration of i, v is equal to $\exp(-e\Psi/kT)$ which is the Boltzmann correction for ions at potential Ψ, x_0 is the distance of closest approach to the adsorbed surfactant layer, and z_i is the charge on ion i.

Through use of the Poisson relation

$$d^2\Psi/dx^2 = \tfrac{1}{2}d(d\Psi/dx)^2/d\Psi = -4\pi\rho_e/DD_o \qquad (16)$$

where ρ_e, the net charge density, is

$$\rho_e = \sum_i n_{\infty i}(v^{z_i} - 1) \qquad (17)$$

Equation 15 becomes

$$\Gamma_i/n_{\infty i} = -kT/(e(8\pi kT/DD_o)^{\frac{1}{2}}) \int_{v_o}^{1} \frac{(v^{z_i} - 1)dv}{v(\sum_i n_{\infty i}(v^{z_i} - 1))^{\frac{1}{2}}} \qquad (18)$$

Here e is the electronic charge, T is the absolute temperature, k is Boltzmann's constant, and v_0 is the value of v at $x=x_o$.

D is the dimensionless dielectric constant of the solvent; D_o, based on the permittivity of free space, is 1.112×10^{-12} coul/volt·cm.

To determine v_o, it is necessary to equate the surface charge to the integral of the diffuse charge of the double layer:

$$\Gamma_s z_s e = \int_{x_o}^{\infty} \rho_e dx \tag{19}$$

where s indicates the surfactant. Substituting the Poisson expression, Equation 17, gives

$$\Gamma_s z_s e = (DD_o/4\pi)(d\Psi/dx)_{x=x_o} \tag{20}$$

$$\Gamma_s z_s e = (8\pi kT/DD_o)^{\frac{1}{2}} (\Sigma_i n_{\infty i} (v_o^{z_i} - 1))^{\frac{1}{2}} \tag{21}$$

With v_o determined from Equation 21, Equation 18 can be evaluated. The relative adsorption for two components is then defined as

$$\beta = \frac{\Gamma_1/n_{\infty 1}}{\Gamma_2/n_{\infty 2}} = \frac{\int_o^{\prime} (v^{z1} - 1)dv/v(\Sigma n_{\infty i}(v^{zi} - 1))^{\frac{1}{2}}}{\int_o^{\prime} (v^{z2} - 1)dv/v(\Sigma n_{\infty i}(v^{zi} - 1))^{\frac{1}{2}}} \tag{22}$$

This equation predicts adsorption preference for the ion of higher charge at equal concentrations.

The analysis is extended to different-sized ions by allowing different distances of closest approach, although the charges are still considered as point charges. The

distance of closest approach is associated with the Stokes radii. Figure 3 presents a physical picture of the hypothetical interface in which a surfactant monolayer of charge z_s is formed at x=0, a layer of small counterions with charge z_1 is formed no closer than $x_{o'}$, and a layer of larger counterions with charge z_2 is formed no closer than $x_{o''}$.

For a binary cationic system, the relative distribution factor as defined in Equation 22 becomes

$$\beta = (\int_{v_{o'}}^{v_{o''}} (v^{z1} - 1)dv/(v(n_{\infty 1}(v^{z1} - 1))^{\frac{1}{2}}) + \int_{v_{o''}}^{1} (v^{z1} - 1)dv/(v(\Sigma n_{\infty i}(v^{zi} - 1))^{\frac{1}{2}}))/(\int_{v_{o''}}^{1} (v^{z2} - 1)dv/(v(\Sigma n_{\infty i}(v^{zi} - 1))^{\frac{1}{2}})) \quad (23)$$

In order to evaluate this expression, the values of $v_{o'}$ and $v_{o''}$ must be determined. As before, the diffuse charge is integrated and equated with the surface charge:

$$\Gamma_s z_s e = (-DD_o/4\pi)((d\Psi/dx)^{<}_{x_{o''}} - (d\Psi/dx)_{x_{o'}} + 0 - (d\Psi/dx)^{>}_{x_{o''}}) \quad (24)$$

Provided the potential variation is continuous, Equation 24 becomes

$$\Gamma_s z_s e = -DD_o/4\pi (d\Psi/dx)_{x=x_{o'}} \quad (25)$$

from which $v_{o'}$ may be evaluated by substituting

$$(d\Psi/dx)_{x_{o'}} = (8\pi kT/DD_o)^{\frac{1}{2}}(n_{\infty 1}(v_o{}^{z1} - 1))^{\frac{1}{2}} \quad (26)$$

In the region $x_{o'} < x < x_{o''}$, Equation 26 may be integrated

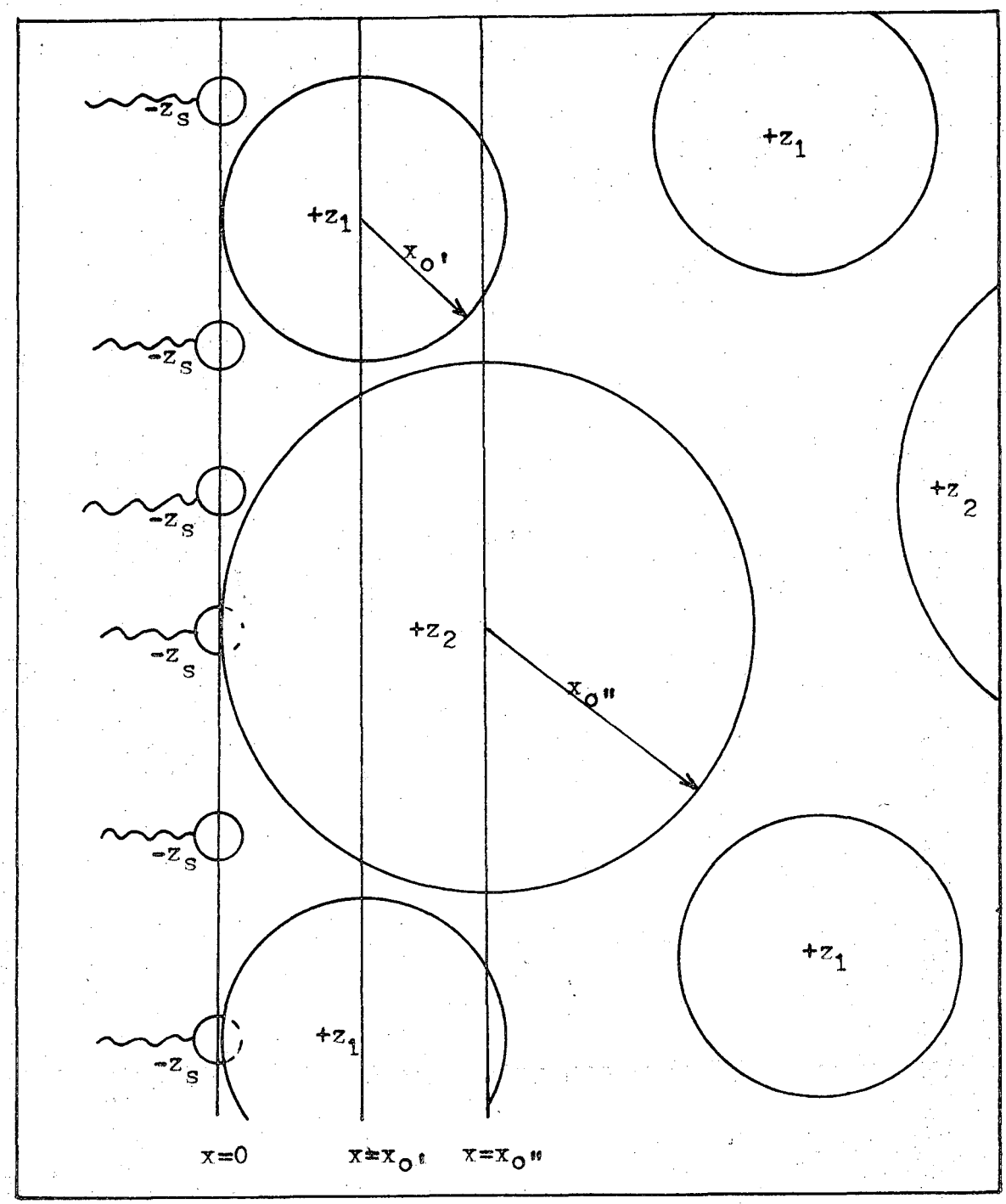

Figure 3. Surface adsorption model for small ions of charge z_1 and large ions of charge z_2 to monolayer of surfactant z_s at x = 0.

analytically, and the result is

$$(-e/(kT))(8\pi kT/(DD_o))^{\frac{1}{2}} n_{\infty_1}^{\frac{1}{2}} (x_{o''} - x_{o'}) = \tan^{-1}(v_{o''}^{z_1} - 1)^{\frac{1}{2}} - \tan^{-1}(v_{o'}^{z_1} - 1)^{\frac{1}{2}} \qquad (27)$$

from which $v_{o''}$ may be evaluated. Jorné's theory shows qualitative agreement with the results of Wace and Banfeld (W2) for cases where data on hydration radii were available. The theory does not take into account the possibility of chelate formation or surface-packing effects. It neglects variations in the dielectric constant, and although it accounts for radius effects its algebra is still based on point charges.

In the development of the charge-interaction theory, several idealizations were adopted in order to make the mathematics tractable. Principal among these is that there are no surface -packing effects and that, except in the case of chelation, there is no specificity for ions except as observed through differences in charge and radius. Investigations of surface-packing effects in rare-earth systems indicate these assumptions may not be entirely valid.

An indication of the behavior of liquid-phase monolayers is given by experimental interactions of rare earths with insoluble monolayers observed through surface-pressure measurements. In interactions between dialkyl phosphates of fourteen, sixteen, and eighteen carbons, light rare-earth

ions up to terbium had little effect on the packing of the monolayer and interacted stoichiometrically with the monolayer species. For the rare-earth ions above terbium, the limiting molecular-surface area was reduced by a third, indicating three-dimensional complexing with the smaller ions of higher charge density. Furthermore, the phosphate film showed selectivity for the heavy rare earths in binary mixed solutions with light rare earths. The fact remains, where charge interactions alone operate, little or no selectivity was observed (H3).

Chelate formation for a metallic ion at a surface requires that the surfactant have at least two functional groups capable of H^+ replacement or coordination, situated so as to form a ring with the cation. Chelate interactions in the surface have not been described by exact mathematical theory, but qualitative conclusions may be drawn from experimental results. Specificity may be ascribed to differences in chelate stability measured by bond strength and thus attributable to differences in the charge-to radius ratio of the metallic species (D2,M1). The influence of surface environment on the stability of chelating bonds, although unexamined, is likely to be an important effect in some systems.

The principal usefulness of theories of chelate formation and charge interaction has been to explain the relative order of adsorption of ions of known dimensions.

In a chelating system both the order of increasing strength of adsorption and the extraction preference should be the same as the order of increasing charge-to-radius ratio; the radii of interest in chelate formation are the crystal ionic radii. In a purely double-layer type of interaction, the order of foam extraction should be the same as the order of increasing charge-to-radius ratio based on the hydrated or Stokes radii. Since the order of increase is opposite for the two kinds of radii, the order of foaming in chelate systems for a series of ions should be opposite to that in a nonchelating double-layer system. It should be noted that the chelate strength may also be affected by surface rearrangements and packing effects.

Foam Density

Identification of the stability of foaming in an apparatus selected for study is essential, because the design considerations given below apply only to stable foaming. For unstable foaming, a comparable hydrodynamic theory has not yet been developed. In the study of foams which behave in an ideal fashion in the sense that they do not coalesce and are still under control of hydraulic effects, several analytical and empirical approaches have been applied to predict the foam density from knowledge of the system parameters.

Haas and Johnson (H1,H2) assumed that the individual Plateau borders (foam lamella intersections through which

the majority of the liquid flow in a foam occurs) could be approximated by small capillaries, and that this flow was described by the Poiseuille relation for axial flow through a right circular cylinder. Their result for vertically flowing foam was

$$f = (k_1 - 1)(32\pi\mu v_s)/(6\rho g d^2) \qquad (28)$$

where v_s is the foam velocity, ρ is the liquid density, μ is the liquid viscosity, and f is the volume fraction of liquid in the foam. The constant k_1 is the value of the ratio of total liquid to Plateau border liquid only and is usually assumed to be 1.5.

Leonard and Lemlich (L1, L2, L4) used the geometry of actual Plateau borders, and by finite-difference procedures were able to solve for the velocity profiles in the borders. These authors were able to predict the flow rate of condensed foam independently of the overall material balances. The procedure requires knowledge or estimation of the surface viscosity and bulk viscosity. Since no coalescence was allowed, the ultimate enrichment was independent of the height of the foam, and the foam density was constant between feed points. The procedure is applicable to columns which are fed directly to the foam as well as to those fed directly to the underlying pool. Their result was

$$f\bar{d}^2 = k_2 v_s^{0.75} \qquad (29)$$

where k_2 is a constant and $\bar{d}^2$ is $\Sigma n_i d_i^3 / \Sigma n_i d_i$. Experimental verification (L3) by the author yielded good agreement.

Rubin et.al. (R5) reviewed the above approaches and evaluated their applicability in several foaming experiments. They found that the Haas and Johnson model agreed better with experimental results than the Leonard and Lemlich model, but that neither model predicted observed dependence on the column diameter. All of their results were correlated by the equation

$$f = k_3 v_s / (\bar{d}^2 D_c^{0.2}) \qquad (30)$$

where D_c is the column diameter.

Flow in stable foams has been correlated recently by

$$f D_{32}^2 = k_4 G^n \qquad (31)$$

where D_{32}^2 is the average bubble diameter and k_4 is a constant. The value of n is 1.0 for plug foam flow (as described in the Lemlich theory) and is 2.5 for turbulent flow in which the foam bubbles are spherical and relatively independent of the foam matrix in their movement. The transition between plug and turbulent flow occurred with increasing gas rate for f lower than 26%; at this value a substantial fraction of polyhedral bubbles were evident. No coalescing foams were observed (R6).

Wace, Alder, and Banfield (W1) considered hydrodynamic behavior to be approximated by a swarm of bubbles rising in a stagnant pool, and derived an expression for the maximum solute throughput as a function of gas velocity and bubble diameter. They found that the solute throughput could be optimized by using the maximum gas rate (the gas velocity before the foam-pool interface disappears), and the optimum bubble diameter of 0.8 mm; at these conditions approximately 165 $cm^2/sec.cm^2$ would be the area throughput.

These authors have considered drainage in a horizontal foam section where the vertical foam velocity is zero. Their result for the exit foam density ϵ is:

$$\epsilon = \epsilon_o \exp(-15.2 + d^2) \qquad (32)$$

where ϵ_o is the foam density at the start of the drainage section, t is the drainage time, and d is the bubble diameter. Haas and Johnson (H2) also worked with horizon al foams and derived theoretical expressions for the foam density based on their capillary model of the Plateau border.

These hydrodynamic theories and correlations find no application to extremely dry or severely coalescing foams; for these foams the only alternative is to perform experiments in order to determine the foam density at the column exit. For extremely dry foams, the liquid flow in the foam may have stopped (the foam has solidified). For coalescing foams,

the bubble size and distribution change so drastically that any attempt to make an exact analysis would be difficult.

There is no priori way to determine how a given system will foam because foaming is a result of such a complex combination of chemical and physical factors. For the purpose of investigating process possibilities, experimental work at an early and indeed at every stage of development is essential.

Separation Problem: The Rare Earth Elements

A particularly interesting and potentially useful application of foam fractionation is to the separation and extraction of the rare-earth elements. These elements (atomic numbers 57 to 71) have been difficult to separate, and consequently, the cost of the individual elements has been prohibitively high (A2.B2).

Uses of the Rare Earths. Current interest in the rare earths stems from their present and anticipated usefulness in medicinal, metallurgical, and industrial applications. The salts of the rare earths are used in embalming to prevent blood coagulation; neodymium sulfoisonicotinate is a thrombosis preventative (K3); and cerium oxalate is an antinausea pharmaceutical. The rare earths have found use as catalysts in ammonia synthesis, esterifications, halogenations, and hydrogenations. They are used as glass-polishing compounds, ultraviolet absorbers in glass, and for imparting

color to glass (S10). Their high thermal-neutron cross-section makes them excellent absorbers in nuclear reactor cores, and they have been employed in a neutron-absorbing paint (P1). The largest user of purified rare earths has been the television industry which uses Eu_2O_3 as a red phosphor in color-television tubes.

Separation Difficulty. The difficulty of separation of the rare-earth ions arises from a similarity in electronic structure, the lack of a variety of oxidation states, and a high degree of hydration. All the rare earths possess completed 5s and 5p orbitals, and differ in the number of electrons in the 4f orbital as shown in Table II. Filling of these orbitals is observed by the radius which decreases with increasing atomic number--the lanthanide contraction.

With a few exceptions, all of the rare earths commonly occur as trivalent ions. The exceptions are Ce, Pr, Tb, Nd, and Dy which also have quadrivalent forms; and Eu, Sm, Yb, Th, and Nd, which may occur in divalent form. In solution only the trivalent species of the rare earths and the quadrivalent form of Ce are observed.

Through hydrolysis, the lanthanons form the aquo complex $M(OH_2)_n^{+3}$ where n is larger than six and may be as high as nine (S11). The hydrated radii increase with increasing atomic number.

Table II. Outer electronic structure and crystal radii of the lanthanides.

element	atom	M^{2+}	M^{3+}	M^{4+}	crystal radius (Å)	change from preceding element (Å)
La	$5d6s^2$	---	(Xe)	---	1.061	
Ce	$4f^2 6s^2$	---	4f	(Xe)	1.034	0.027
Pr	$4f^3 6s^2$	---	$4f^2$	4f	1.013	0.021
Nd	$4f^4 6s^2$	$4f^4$	$4f^3$	$4f^2$	0.995	0.018
Pm	$4f^5 6s^2$	---	$4f^4$	---	0.979	0.016
Sm	$4f^6 6s^2$	$4f^6$	$4f^5$	---	0.964	0.015
Eu	$4f^7 6s^2$	$4f^7$	$4f^6$	---	0.950	0.014
Gd	$4f^7 5d6s^2$	---	$4f^7$	---	0.938	0.012
Tb	$4f^9 6s^2$	---	$4f^8$	$4f^7$	0.923	0.015
Dy	$4f^{10} 6s^2$	---	$4f^9$	$4f^8$	0.908	0.015
Ho	$4f^{11} 6s^2$	---	$4f^{10}$	---	0.894	0.014
Er	$4f^{12} 6s^2$	---	$4f^{11}$	---	0.881	0.013
Tm	$4f^{13} 6s^2$	$4f^{13}$	$4f^{12}$	---	0.869	0.012
Yb	$4f^{14} 6s^2$	$4f^{14}$	$4f^{13}$	---	0.858	0.011
L Lu	$4f^{14} 5d6s^2$	---	$4f^{14}$	---	0.848	0.010

Only the valence shell electrons, that is, those outside of the (Xe) shell, are given. A dash indicates that this oxidation state is not known in any isolable compounds.

Orbitals: H.H. Sisler, C.A. VanderWerf, A.W. Davidson, General Chemistry, 2nd ed., (Macmillan Co., New York 1959), p.681.

Radii: F.A. Cotton, G. Wilkinson, Advanced Inorganic Chemistry (Interscience, New York, 1962), p.870.

Separation Methods for the Rare-Earth Elements. The chemistry of the rare earths is largely ionic, and classical separations of them have been based on ionic interactions. Because of the previously mentioned factors, these separations have not been very specific. The main industrial unit operations have been basicity separations and precipitation of sulfates, double sulfates, oxalates, fluorides, and carbonates. Even with the advent of more advanced methods to be discussed below, "all recently published schemes--without exception--for the separation of the rare-earth elements are based upon the elimination of the bulk of the major elements (cerium and lanthanum in the cerium subgroup, yttrium in the yttrium subgroup) by "classical" methods. Europium, samarium, and ytterbium are recovered by valence change reactions. Ion exchange methods are always employed, but only after preliminary enrichment by other means..." (B2). The details of the classical methods are indicated in the excellent review by H.E.Kremers (K3).

Recent large-scale separations make use of complexing and chelating agents as separating agents, because they penetrate into the hydration spheres of the lanthanons and result in greater specificity than is observed through ionic interactions. The strength of each chelate is governed by ionic charge, ionic radius, basic strength, steric hindrance for ring formation, ring size, and the number of rings. For a

given chelating agent and for like-charged ions, the order of chelate stability of rare earths increases from La to Lu in the same direction as decreasing crystal radius and increasing basicity. Separations have been performed using chelating agents as precipitating agents and in ion exchange (P4,T1,W5).

Ion-exchange separations of the rare earths are of two types. Elution chromatography employing chelating agents as elutants is of interest in analytical applications, but uneconomical otherwise. Displacement chromatography, employing EDTA or other chelating agents as elutants and ammonium or alkali-metal ions as displacement ions, is capable of producing ton-sized quantities of pure rare earths (P3). Table VI shows theoretical single-stage separation factors for each of the adjacent rare earths in a displacement-chromatographic separation using EDTA as the elutant (P4). These values range from 1.1 for the Gd-Eu separation to 4.2 for the Tb-Gd separation. The average separation factor was 2. EDTA provides good separation of all the lanthanons but is restricted somewhat by its low solubility.

Tompkins (T1) found that in separations using Dowex 50, rare earths should not exceed 3×10^{-4} M in rare earth; using Amberlite IR-1, the concentration should be 10^{-6} M or less. Several different eluting agents have been employed (S11); EDTA was considered to be the most effective. Other elutants used were hydroxyacids, amion acids, and amino-polycarboxylic

acids. All ion-exchange-related separation techniques are limited by not being continuous.

Much recent interest has been focussed on liquid-liquid extraction of the rare earths using phosphorus-based extractants. Most commonly mentioned has been TBP, tri-n-butyl-phosphate, which extracts nitrate-complexed rare earths from concentrated nitric acid solutions. Extraction by monoacidic phosphates and phosphonates displayed larger separation factors, but was complicated by precipitation phenomena (W6).

Molybdenum Corporation of America (Molycorp), which is currently the largest producer of rare-earth products in the United States, uses a liquid-liquid ion-exchange process for the separation of rare-earth oxides. The process has the capability of producing 10 tons of europium oxide annually at 99.9% purity (M5).

The search for better rare-earth separation methods has largely been in the direction of

(a) eliminating the limitations imposed by the need to exceed the solubility product,

(b) eliminating the limitation imposed upon the ultimate purity by carrying of a contaminant rare earth,

(c) enhancing the single stage difference between a given pair of rare earths, and

(d) trying to achieve the multiplication of stages more readily.

The ion-exchange technique has made major improvements in the first three of these criteria; if it is operated in the batch mode, improvement is achieved in all four.

Liquid-liquid extraction meets all four requirements but is limited since the utilization of more that 20 stages (countercurrently) is frequently difficult (P5).

Foam fractionation would seem to satisfy a,b, and d without question and is readily operated continuously. Its potential usefulness will depend on its ability to satisfy the requirement of single-stage enhancement, and this will depend in turn on the extent of multiple contacting in the foam.

Application of Foam Fractionation in Ion Extractions and Separations

Much of the recent research with foam fractionation has been applied to the extraction of surface-inactive metal ions by surface-active counterions. These extractions have demonstrated selectivity based on charge interactions and on chelate formation in a wide variety of systems. Although some attention has been focussed on rare-earth elements, no attempt has been made to separate between rare-earth ions by the method. Table III summarizes the research by listing the metallic ions extracted from solution, the extracting surfactant, and the ions from which a selective separation was made if other than sodium. The table includes a listing of

Table III. Foam fractionation of metallic ions.

ion in foam	retained ion*	surfactant**	references
Ag^{+}		a	W4
Al^{+3}	Sc^{+3}	e,AS	B1
Ca^{+2}		a	W4
Ca^{+2}	Cs^{+1}	b	W1,W2
Ce^{+3}	Cs^{+1}	b	W1,W2
Ce^{+3}	Sc^{+3}	e,AS	B1
Co^{+2}		h,i,j,k	S4
Cs^{+}		a,d,e,f,g,l,m,n,o,p,q, r,s,t,u,v,w,x,y,z,AA, AB,AC,AD,AF,AP,AQ,AR	S5
Cs^{+}	Ce^{+3}, Ca^{+2}, Sr^{+2}, Th^{+4}	b	W1,W2
Cu^{+2}			R4
Cu^{+2}		AD	R1
Fe^{+3}		a	W4
Fe^{+3}		AD	R1
Fe^{+3}	Sc^{+3}	e,AS	B1
H^{+}		a	W4
K^{+}		a	W4
La^{+3}		AG	S2
Mg^{+2}		a	W4
Mn^{+2}	Sc^{+3}	e,AS	B1
Na^{+}		a	W4

(table continued on next page)

ion in foam	retained ion*	surfactant**	references
Na^{+}	Sc^{+3}	e,AS	B1
NH_4^{+}		a	W4
Ra^{+2}		h,i,j,k	S4
Ra^{+2}	Ca^{+2}, U^{+3}, Na^{+}	c,d,e,f,g,h	S3
Sc^{+3}	$Na^{+}, Mn^{+2}, Fe^{+3}, Al^{+3}, Ce^{+3}, V^{+3}, U^{+3}$	e,AS	B1
Sm^{+3}		h,i,j,k	S4
Sm^{+3}		a,d,e,f,g,l,m,n,o,p,q, r,s,t,u,v,w,x,y,z,AA, AB,AC,AD,AF,AP,AQ,AR	S5
Sm^{+3}	Sr^{+2}	(see reference S5 above)	S5
Sr^{+2}		AH,AO,v,p,o	S1
		f,AE	S2
		b	W3
Sr^{+2}	Cs^{+}	b	W1,W2
Sr^{+2}	Sm^{+3}	(see reference S5 above)	S5
Th^{+4}	Cs^{+}	b	W1,W2
Th^{+4}	UCl_5^{-2}	AL,AM,AN	J2
U^{+3}	Sc^{+3}	e,AS	B1
UCl_5^{-2}	Th^{+4}	AL,AM,AN	J2
$U(CO_3)_5^{-2}$	$V(CO_3)_5^{-2}$	AI,AJ,AK,AL	J1
UO_2^{+2}		AE	W4
$V(CO_3)_5^{-2}$	$U(CO_3)_5^{-2}$	AI,AJ,AK,AL	J1
V^{+3}	Sc^{+3}	e,AS	B1
Zn^{+2}		a	W4
Zn^{+2}	H^{+}	AT	K2

* retained ion is Na^{+} in cases where no other ion specified.
** key to surfactants is given on following pages.

Table III continued. Key to surfactants.

key	common name	chemical name	chemical structure
a	PMT	palmitoylmethyltaurine	$C_{15}H_{31}CON(CH_3)CH_2CH_2SO_3Na$
b	NaDBS	sodium dodecylbenzene sulfonate	$C_{12}H_{25}C_6H_4SO_3Na$
c	Sipon LT-6	triethanolamine laurylsulfate	$C_{12}H_{25}N(CH_2CH_2OH)_3SO_4$
d	Aerosol-22	tetrasodium N-(1,2-dicarboxyethyl) N-octadecylsuccinamate	$C_{18}H_{37}N(CH(COONa)CH_2COONa)-(COCH_2S(CHCOONa)O_3Na$
e	Igepon TC-42	sodium N-methyl-N-coconut oil acid taurate	$C_{19}H_{22}CON(CH_3)CH_2CH_2SO_3Na$
f	Tergitol-7	sodium sulfate of 3,9diethyltridecanol	$C_4H_9CH(C_2H_5)C_2H_4CH(SO_4Na)-CH_2CH(CH_3)_2$
g	DBDTTA	dodecyl-benzyldiethylenetriamine tetra-acetic acid	$C_{12}H_{25}C_6H_4CH_2N(CH_2COONa)CH_2-CH_2N(CH_2COONa)CH_2CH_2N(CH_2COONa)_2$
h	Nacconol 60s	alkylarylsulfonate	
i		toluene sulfonate	$NaSO_3C_6H_4CH_3$
j		alkylsulfosuccinates	$NaSO_3CHCOORCH_2COOR'$
k		coco-oil acid laurates	
l	Areskap 100	aromatic sulfonate	
m	Alipal CO-436		$RC_6H_4(CH_2CH_2O)_4SO_4NH_4$

Key to surfactants continued.

key	common name	chemical name	chemical structure
n	Aerosol OT	sodium dioctylsulfosuccinate	$NaSO_3CH(COOC_{18}H_{37})CH_2COOC_{18}H_{37}$
o		lauryl-B-alanine	$C_{12}H_{25}NH_2CH(CH_3)COONa$
p	Deriphat 160	dodecyliminodipropionic acid	$CH_3(CH_2)_{10}CON(CH_2CH_2COOH)_2$
q	Deriphat 170	aminocarboxylic acid	
r	DIDAA	dodecyliminodiacetic acid (sodium salt)	$CH_3(CH_2)_{10}CON(CH_2COONa)_2$
s	Dowfax 2A1	dodecyldiphenyloxidedisulfuric acid	
t	Igepon T43	sodium N-methyl-N-olelyltaurate	$C_{17}H_{33}CON(CH_3)CH_2CH_2SO_3Na$
u	Igepon TN-74	(see a)	
v	Maypon K	polypeptide	
w		N-dodecylbenzyldiethylenetriamine triacetic acid	$C_{12}H_{25}C_6H_4N(COOH)CH_2CH_2N(COOH)_2$
x	Triton-100		$RC_6H_4(CH_2CH_2O)_5OH$
y	Triton-200	sulfonated polyethylene oxide	
z	Ultrawet		$C_6H_4RSO_3Na$
AA	Victawet 58-B	phosphorated capryl alcohol	$(capryl)_5(P_3O_{10})_2$

Key to surfactants continued.

key	common name	chemical name	chemical structure
AB		sodium oleate	$C_{17}H_{33}COONa$
AC		sodium laurylsarcosinate	$C_{11}H_{23}CON(CH_3)CH_2COONa$
AD		sodium laurylsulfate	$C_{11}H_{23}CH_2SO_4Na$
AE	Aresket 300		
AF	Miranol 2MCA		$C_{11}H_{23}C(-)NCH_2CH_2N(-)(OSO_3C_{12}H_{25})(CH_2COONa)CH_2CH_2OCH_2COONa$
AG	RWA-100		
AH	Bacto-tryptose	protein digest mixture	
AI	Ammonyx TRM	cetyltrimethylammonium chloride	$C_{16}H_{33}N(CH_3)_3Cl$
AJ	Aliquat 336	decyltrimethylammonium chloride	$C_{10}H_{21}N(CH_3)_3Cl$
AK		cetyldimethylbenzylammonium chloride	$C_{16}H_{33}N(CH_3)_2(C_6H_5)Cl$
AL	Hyamine 1622	diisobutylphenoxyethoxyethyl-dimethylbenzylammonium chloride	$((CH_3)_3CCH_2C(CH_3)_2\ C_6H_4OCH_2CH_2OCH_2CH_2N(CH_3)_2CH_2C_6H_5)Cl\cdot H_2O$
AM	Ammonyz	stearyldimethylbenzylammonium chloride	$C_{17}H_{35}N(CH_3)_2Cl$

Key to surfactants continued.

key	common name	chemical name	chemical structure
AN		cetyldimethylbenzylammonium chloride	$C_{16}H_{33}N(CH_3)_2(C_6H_5)Cl$
AO		sodiumoleate (see AB)	
AP	Intramine Y		$RCONHCH_2CH_2OSO_3Na$
AQ	Miranol CM		$C_{11}H_{23}C(-)NCH_2CH_2N(-)(CH_2CH_2-ONa)_2OH$
AR	Nekal 75		$C_4H_4C_6H_3RSO_3Na$
AS	DBS	dodecylbenzenesulfonic acid	$C_{12}H_{25}C_6H_4SO_3H$
AT		sodiumalkylbenzensulfonate	$RC_6H_4SO_3Na$

the surfactants with their chemical and commercial names.

Selectivity Among Divalent and Monovalent Metal Ions. In an extensive study of the foam fractionation of various divalent and monovalent ions, an order of selectivity based on the strength of adsorption of individual ions was found by Walling (W4). In the divalent series, Mg^{++} was more strongly adsorbed than Ca^{++}; in the univalent series, the order of decreasing adsorption was $NH_4^+ > K^+ > Na^+ > H^+$. Both series were formulated from experiments where the ions were foamed individually, at different concentrations, from solutions of PMT (palmitoyl methyl taurine), and thus the conclusions drawn about relative selectivities may be in error. In Walling's results, divalent-ion separation varies inversely with the crystal ionic radii and thus with bonded chelate interaction; whereas, monovalent-ion separation varies nearly inversely with the Stokes radii, i.e. the hydrated radii, and thus appears to depend on charge interaction in the surface layer. Table IV reports crystal and Stokes radii used above.

Separations of Metal Ions from Rare Earth Ions. The separation of Cs^+ from Sr^{++}, Ce^{+3}, Th^{+4}, and Ca^{++} resulted in the following molar adsorption ratios in the foam: $Sr^{++}/Cs^+ = 55$, $Ca^{++}/Cs^+ = 38.5$, $Ce^{+3}/Cs^+ = 3.7$, and $Th^{+4}/Cs^+ = 1.5$ (W1, W2). The excessive suppression of the highly charged species of cerium and thorium was explained on the basis of steric hindrance at the two dimensional interface. It was noted

Table IV. Crystal and Stokes ionic radii for selected cations.

cation	crystal radii (A)	Stokes radii (A)
H^+	----	0.253
Na^+	0.95	1.80
K^+	1.33	1.21
NH_4^+	1.48	1.275
Mg^{++}	0.78	1.725
Ca^{++}	1.06	1.53

Crystal radii: R.C. Evans, An Introduction to Crystal Chemistry (Cambridge University Press, Cambridge, 1966).

Stokes radii: E.A. Moelwyn-Hughes, Physical Chemistry, 2nd ed., (Pergamon Press, New York, 1961).

that in comparable ion-exchange and solvent-extraction processes, the separation between Cs^{+} and the other ions increased with increasing valence.

Foam fractionation of radioactive species to reduce contamination in dilute plant wastes has been reported in several articles (S1, S2, S4, S5). In the most complete of these (S5), three surfactants--dodecyliminodipropionic acid (Deriphat 160), dodecyliminodiacetic acid (DIDAA), and dodecylbenzyldiethylenetriamine tetra-acetic acid (DBTTA)--were applied to the separation of Sm^{+3} from Sr^{++}. Hydroxide competition with the surfactant was observed at pH values over 6.0 for Deriphat 160 and DIDAA, and caused samarium adsorption in the foam to be depressed; rare-earth hydroxides precipitate near and above pH=6 (M2). DBTTA showed evidence of chelate formation since adsorption of both samarium and strontium increased as the pH increased to values above 7 where hydroxide formation ordinarily depressed extraction. In all acid solutions, samarium was preferentially adsorbed from solutions 10^{-6} M in Sm^{+3}, 10^{-5} M in Sr^{+3}, 1.0 M in $naNO_3$, and 0.2 to 0.4 gm/l in surfactant.

Extraction of Rare Earth Elements. The enrichment of La^{+3} with the commercial surfactant RWA-100 was strongly dependent on the pH as reported by Schoen (S2). Maximum enrichment occured at about pH 4.5. At higher pH, competition with $La(OH)_3$ precipitation was experienced; and at

lower pH, competition with the acid form of the surfactant was experienced. This type of pH dependence is typical of metal ions and was reported by Schoen for Sr^{++} and UO_2^{++} as well.

In studying the extraction of Sc^{+3} by dodecylbenzene sulfonic acid (SA) and sodium n-methyl-n "coconut oil acid" taurate (MT) from solutions 10^{-4} M in Sc^{+3}, Bauer (B1) found enrichment ratios as high as 6.5 at gas flowrates of 25ml/min. Other ions competed strongly for surface positions, although SA showed some preference for Sc in the presence of Ce. High temperature (70°C) improved enrichment by lowering the surface tension; adjusting the pH to 5.0 yielded the maximum enrichment of Sc.

STATEMENT OF THE PROBLEM

Foaming separations by stable (persistent or noncoalescing) foams are well established in the literature. The properties and characteristics of unstable (transient or coalescing) foams have not received the same attention. Nevertheless, foaming in the transient mode may be necessary if the system will not form a persistent foam, and may be desirable if the maximum enrichments and extractions are obtained in this mode. In transient foaming, the coalescence of foam bubbles results in surface-area decrease with increasing height in the foam layer. It should create an internal reflux of material displaced from the rapidly shrinking area, and should thus promote a foaming extraction and separation of materials such as the rare-earth elements, by producing a multiplication of stages within a single contacting unit. An experimental program was therefore undertaken to examine transient foaming from several different aspects.

Surfactant Extraction

Anionic surfactants merit particular study because of their potential salt-forming capacity in metal-cation adsorption. For this reason an exploratory study was carried out to determine extraction efficiencies and rates for such a surfactant, over widely varying gas rates and at two solution-phase concentration levels, in apparatus of fixed foam height.

Rare-Earth Separation

An extraction system was adopted in which the selectivity property for rare-earth elements was provided by a chelating agent, and the foaming and extracting function was supplied by a cationic surfactant. Measurements were made to determine the effects of concentration levels of surfactant, complexing agent, rare-earth ions, and pH on the nature of the foaming separation, mode of faaming, and effectiveness of the separation and extraction. It was desired to determine whether ion flotation, precipitate flotation, or foam fractionation would occur, and to find means of controlling the foam stability and wetness so as to maximize the separation capactiy.

The preliminary studies indicated that residence time in the foam column controls the specific liquid content and separating capacity, and hence that foam height, gas flow rate, and column diameter need not be varied separately. It proved convenient to adopt a constant relatively low, gas flow rate for all runs, and to vary the foam height over a substantial range.

Cerium-neodymium and cerium-samarium mixtures were selected as typical systems for foam-separation trials, as being relatively difficult to separate and relatively easy to analyze. Because separation rather than complete removal was the postulated objective, a steady-state continuous-flow operation was adopted.

EXPERIMENTAL PROGRAM

Apparatus

In order to determine the practicality of a foam for separations, it was necessary to study foams formed under various contrived conditions. These conditions were both chemical and physical, and included such variables as species concentration, pH, gas flowrate, and foam height.

An apparatus was constructed in which the chemical effects could be studied and which itself provided for the physical effects. Since this apparatus was both an experimental tool and a prototype of production equipment, it had to provide for visibility, versatility, easy cleaning, and easy assembly. All of these criteria were met by using a tall, 50mm diameter glass pipe fitted at the bottom with a a gas-bubbling device and at the top with a means of removing and collecting foam . This glass pipe or foaming column is illustrated in Figure 4 and was constructed of removable sections gasketed with O-ring joints.

The top or foam-exit section featured a diameter reduction from 50mm to 4mm. A piece of 4mm glass tubing connected to the top carried the foam to a suitable receiving vessel.

The next section or feed section was provided with a 4mm inlet tube. In all of the experiments, the pool-liquid interface with the foam was maintained just above the feed inlet.

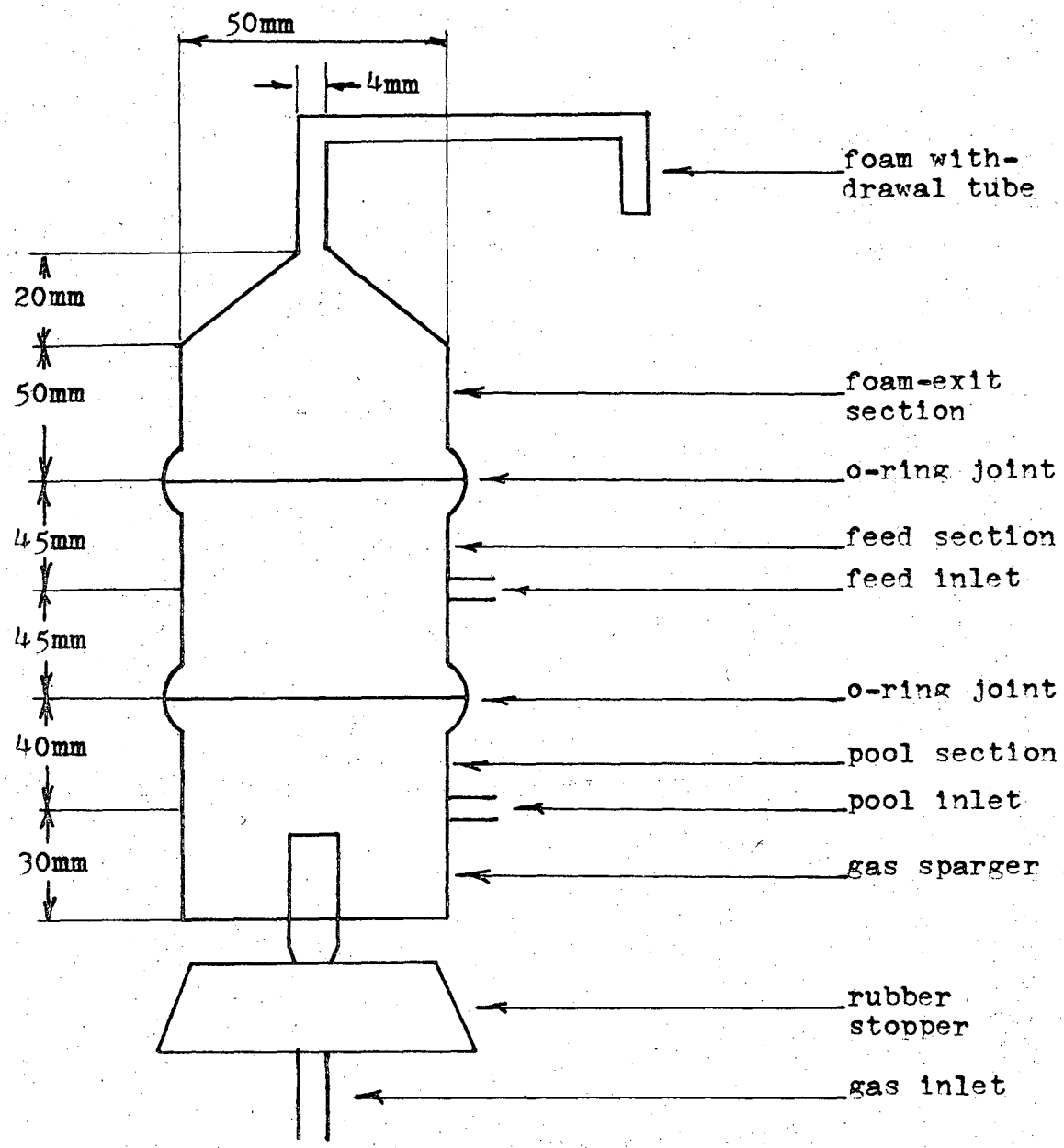

Figure 4. Foaming column (not to scale).

The bottom or pool section was provided with a 4mm inlet tap and a gas bubbling device. The pool section was open at the bottom, and N_2 was added through an extra-coarse-grade sintered-glass sparging tube, which was inserted through a rubber stopper placed in the open bottom. This section was easy to clean and would allow for rapid substitution of other gas-bubbling devices.

Foam drainage was provided for in the 10cm height between the liquid-foam interface in the feed section and the top of the foam-exit section. Greater drainage lengths could be studied merely by inserting glass extensions between the foam-exit and the feed section. In actual practice, 18, 24, and 33cm foams were also used. The pool volume was about 200ml.

This column was always operated with continuous foam, feed, and pool streams.

A 25mm diameter glass column was used in early developmental work and for the foaming of the anionic surfactant Aerosol 22. The column was constructed in two sections, a foam exit section and a pool section, connected at an O-ring joint. The pool section featured two 4mm taps, one for feed

and one for pool drawoff, and an extra-coarse-grade sintered-glass disk for gas bubbling. The foam exit was similar to the 50mm-column exit in providing a sharp reduction in diameter at the column top. Foam drainage in this column occurred in the fixed 6cm height between the pool surface and the beginning of the exit constriction. Liquid volume of the pool was 60ml.

This column was also operated only with continuous feed and continuous foam and pool offtake.

Several reflux-inducing devices were provided for the 50mm column. These included a Mylar disk perforated with 150 holes of 0.75mm diameter, equally spaced over the disk cross-section. The surface of this disk which was roughened by perforation at the edges of the holes faced downward in the column. Other devices tested were a 60mm deep packing of 9mm plastic beads, a single 30-mesh stainless steel screen, a compact stack of three 30-mesh stainless screens, a single 18-mesh plastic screen, and a single 100-mesh stainless steel screen. The devices were inserted at joints between major sections of the foam column.

Auxiliary Equipment. Auxiliary components for the column are indicated in the schematic diagram of Figure 5. These included a constant-head feed-liquid tank, liquid rotameter, N_2 source, feed-gas humidifiers, manometer, and a bubble counter for measuring the gas flow rate. Most of

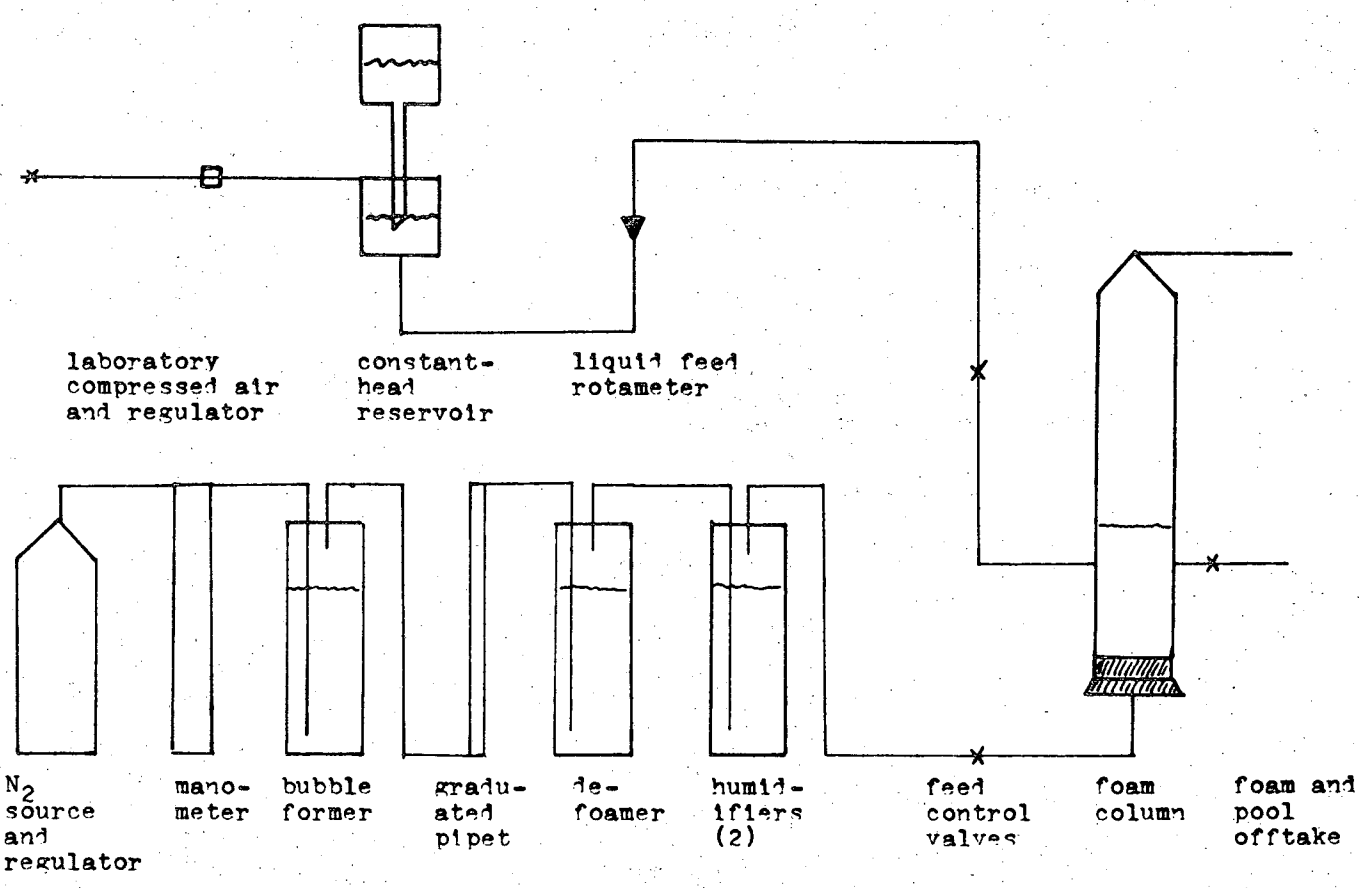

Figure 5. Schematic of complete foaming apparatus.

these apparatus were of standard design and need no further description. The bubble counter, however, was a 10.00-ml pipet mounted between two gas bubblers: the upstream bubbler containing an aqueous solution of a foaming surfactant, Igepon AP-78 (GAF Corporation), and the downstream bubbler containing an aqueous solution of a defoaming agent, Antifoam 60 (General Electric Co.). Volumetric flow was measured by timing the passage of a bubble lamella between marked divsions on the pipet.

Chemicals

The chemical reagents used in the foaming experiments included three rare-earth chlorides and two surfactants. Table V presents a listing of these chemicals, their commercial and chemical names, chemical structures, molecular weights, and the commercial source from which they were obtained. Concentrated (2.5g/l) stock solutions of the lanthanide chlorides (Ce,Nd,Sm) were prepared directly from the supplied reagents. The $SmCl_3$ stock solution required mild acidification with HCl to completely dissovve the salt. Feed solutions were prepared by adding small volumes of the stock solution to a suitable volumetric container. Distilled water and any other solution components were then added and the entire solution mixed thouroughly. Feed pH was adjusted with dilute HCl.

The laboratory supply of distilled water was deionized by treatment with a Barnstead #0802 ion-exchange cartridge.

Table V. Chemicals used in foam-fractionation studies.

chemical name	commercial name	structure	molecular weight	supplier
cerous chloride		$CeCl_3$	246.5	K&K Laboratory
neodymium chloride		$NdCl_3$	250.6	K&K Laboratory
samarium chloride		$SmCl_3$	254.6	Bryant Laboratory
tetrasodium N-(1,2-dicarboxyethyl)-N-(octadecylsulfosuccinamate	Aerosol 22 (35%)	$C_{18}H_{37}N(CHCOONa-CH_2COONa)(\bigcirc CCH_2-CHSO_3NaCOONa$	653	American Cyanamid
diisobutylphenoxyethoxyethyldimethylbenzylammoniom chloride monohydrate	Hyamine 1622	$((CH_3)_3CH_2C(CH_3)_2-C_6H_4OCH_2CH_2OCH_2CH_2-N(CH_3)_2CH_2C_6H_5)^+Cl^-\cdot H_2O$	466.1	Rohm & Haas
ethylenediaminetetraacetic acid (disodium salt)	EDTA	$(HOOC)_2NCH_2CH_2N-(COONa)_2$	372	K&K Laboratory

Two surfactants were used for foaming. The anionic compound used, Aerosol 22, has an eighteen-carbon-chain hydrophobic portion, and a hydrophilic part comprised of three carboxylates and one sulfonate group.

The cationic surfactant studied was a quaternary ammonium salt, Hyamine 1622, containing a long chain with both aryl and alkyl groups, and two ether linkages.

The chelating agent EDTA contains four carboxylate ions available for chemical bonding. Its disodium salt form yields a singly charged negative ion in combination with the tripositive rare-earth ions.

Procedures

Criteria for Selecting Operating Conditions. Liquid flow rates were selected that would allow the pool to remain essentially undepleted during the foaming experiments. A volumetric feed rate approximately 100 times the condensed-foam volumetric rate was considered sufficient for this purpose.

Gas flow rates and most solute concentrations were considered as experimental variables. The only criterion for the latter was that the total rare-earth concentration be in excess of the complexed rare-earth concentration to a sufficient degree for the system to show specificity.

Equipment Operation and Experimental Procedures. Prior to each new experiment, the entire apparatus was rinsed

thoroughly with deionized water. If the foam-exit section and withdrawal tube appeared cloudy, they were washed also with soap-and-water solutions before the rinsing.

To start a run, the gas flow rate was set, and feed solution was then introduced from the reservoir through process lines, to bring the pool-section level up to 6 or 10cm (for the 25mm or 50mm column respectively). Normally, foam began to form inmediately, above the pool-liquid surface. When the foam first overflowed through the withdrawal tube, the time was recorded, and continuous input and drawout of liquid was begun.

Foam height was defined as the distance from the pool-foam interface to the level in the upper or exit section where the inside diameter first decreases. Other measurements made were gas flow rate, liquid feed rate, and temperature. Notes were taken on the stability of the foam. approximate size of the individual foam bubbles, visible effects of coalescence-promoting divices, and the presence of particulate matter.

Some coalescence of foam occurred during its passage into the collecting vessel, and coalescence was completed by standing for several hours. The total coalesced overflow was then collected, and its exact volume noted. This entire sample was quantitatively transferred into a digestion crucible (as described under Chemical Analysis). The total

pool overflow was also collected, and its exact volume and pH were noted.

Chemical Analysis of Rare-Earth Content

Two analyses were performed on each foam, pool, or feed sample. First, the Ce content was determined by oxidation-reduction titration. Second, total rare earth was established by complexiметric titration with EDTA. Standard samples of Ce, Nd, and Sm were run as checks each time the analyses were performed. The procedures as described here applied to foaming runs with Hyamine 1622.

Sample Preparation. Destruction of complexing agents and surfactant present in the sample was necessary, because of competitive effects of these constitients during the complexiметric titration.

The condensed-foam liquid volume was measured and recorded, and then the sample was quantitatively transferred to a 30ml silica crucible. Soap accumulations on the foam exit downcomer were rinsed off and were added to this crucible. Silica glass was used because of its low content of interfering oxides, such as Al_2O_3.

One to two ml of concentrated sulfuric acid were added to the crucible contents, and the solution was heated slowly (not boiling) in a laboratory hood to evaporate the water content. When the volume was reduced to a few ml, the heating rate was increased to cause both the charring of organic

matter and the evaporation of sulfuric acid. This low-temperature charring prevented any attack on the crucibles by EDTA during subsequent steps of the sample digestion.

The charred sample was ashed in an electric muffle furnace, and the ashed sample was dissolved with heating in one ml of concentrated sulfuric acid. This sample was quantitatively transferred into a 100ml volumetric flask and subsequently split into two or more samples.

Wet oxidation of the organic matter in the samples was attempted using H_2O_2, HNO_3, or fuming HNO_3 but was found unreliable; these oxidizing agents attacked the Pyrex glassware then in use, and the time to carry out the oxidation was excessive. Precautions were also necessary to reduce heating rates near dryness because of possible mild nitrate explosions.

Cerium Analysis(W7). One sample fraction was added to 250ml of a 0.94N sulfuric acid solution, the acid being used to prevent the hydrolysis and precipitation of Ce^{+4}.

To oxidize Ce^{+3} to Ce^{+4}, 5.0 ml of a 0.15N solution of $AgNO_3$ were added as catalyst, followed by approximately two grams of ammonium persulfate as oxidizing agent. The Ce^{+4} solution which has a fairly intense yellow color was boiled gently for 10 to 20 minutes to decompose excess persulfate and was then cooled to room temperature.

To this solution, 50λ of a 0.025M solution of ferroin

indicator, 1,10-(ortho)-phenanthroline ferrous sulphate, were added. This indicator is oxidized from its red form to a colorless form by the Ce^{+4}, and the subsequent titration must account for the indicator blank. $FeSO_4$ in a solution of about 0.02 gm/l was used to titrate the excess Ce^{+4} and oxidized indicator. The Ce^{+4} was reduced before the indicator because it is the stronger oxidizing agent. The endpoint transition was from yellow to colorless to orange, and the orange intensification was followed on a Bausch and Lomb #340 spectrophotometer or a Beckman DU-2 at 505mμ . The endpoint was taken as the point where full orange intensity was reached, as determined from a plot of absorbance versus volume of $FeSO_4$ solution added.

Total Rare-Earth Analysis (S13). The second sample fraction was diluted to about 250 ml with deionized water. A small spatula of ascorbic acid was added to prevent oxidation of indicator by Ce^{+4}. To insure proper color transitions of the indicator and to prevent precipitating hydroxides, the pH was adjusted to 7.5 by adding the needed amount of a 20% solution of triethanolamine (TEA). Sharper transitions in color were obtained when the pH of the solution was pH2 or less before adding the TEA.

About 0.15 to 0.20 gms of a solid dilution of the indicator eriochrome black T (EBT or 1(1-hydroxy-2-napthylazo)-6-nitro-2napthol-4sulfonic acid sodium salt) with NaCl

(1 part EBT to 300 NaCl) were added to this solution. The solid dilution of the indicator was necessary because EBT liquid solutions are susceptible to oxidation (W10). The resulting reddish violet solution was titrated to a persistent blue endpoint with a standardized 0.002N solution of EDTA.

Neodymium or Samarium Determination. The amount of Nd or Sm in a given sample was determined by the difference between the observed total rare-earth content and the Ce content.

Physical Analysis for Aerosol-22 Runs.

Aerosol 22 in foam samples was determined by measuring its ultrviolet absorption at 206 mμ in a Beckman DU-2 spectrophotometer.

RESULTS AND DISCUSSION (PART I): GENERAL OBSERVATIONS

This section provides an analysis of both experimental and conceptual aspects of foam fractionation in the transient mode. Its objective is to establish the design considerations necessary for conducting a transient foaming separation, and also to compare transient and persistent foams. The systems examined are the foam extraction of an anionic surfactant, Aerosol 22, and the foam extraction-separation of rare-earth ions.

Surfactant Selection

Interactions with Metal Ions. The foam extraction-separation of nonsurface-active materials (rare-earth ions) requires use of a surface-active substance which can extract ions, distinguish between these ions, and form a foam. The choice of surfactant will depend on both the magnitude of the specificity for the ions and the mode of foaming required.

Essentially, two different types of surfactant/rare-earth interactions can be identified. The first of these, nonbonded interactions as described in the Jorné theory (see Introduction), show specificity for ions as a result of differences in charge or radius only. The preferred surfactant for this type of interaction would probably be one of the large number of anionic univalent surfactants.

The degree of specificity attainable in a nonbonded interaction was determined by numerically evaluating the

Jorné theory for separating between pairs of rare-earth ions over a solution 5×10^{-4} M in total rare earth, with a surfactant surface coverage of 30 A^2/molecule. Differences in radii for the tripositive rare-earth ions were estimated to be comparable to the differences in the crystal radii, about 0.009 Å between adjacent elements. The calculation showed that such a radius difference would yield a separation factor of 1.05 for a very dry foam. This marginal result is believed to disqualify nonbonded interactions from consideration as a potential separating effect. On the basis of this conclusion, the main effort of this work was devoted to seeking optimal conditions for bonded-interaction operation.

In the following paragraphs, algebraic relations will be developed that have proved necessary for interpreting experimental runs involving bonded interactions.

An overall separation factor for the contacting unit is given by

$$\alpha = (c_{as}c_{bs})/(c_{ap}c_{bs}) \qquad (33)$$

where c_a and c_b are the activities (equal to concentrations in dilute foaming solutions) of ions A and B in the foam (s) and pool (p) streams. For the special case in which all of both A and B are complexed with surfactant, unless surface-activity or surface-packing effects occur, the ratio of A to B will be the same in the foam and in the pool, and no separation will occur ($\alpha = 1$).

For the practically significant situation where the concentration of rare-earth ions exceeds that of the surfactant, the separation factor becomes

$$\alpha = (c'_{as}+c_{as})(c'_{bp}+c_{bp})/((c'_{ap}+c_{ap})(c'_{bs}+c_{bs})) \qquad (34)$$

where primes indicate concentrations of complexed substances. For small extents of extraction, the ratio of A to B in the pool matches the feed (a_o/b_o):

$$\alpha = ((c'_{as}+c_{as})/(c'_{bs}+c_{bs}))(b_o/a_o) \qquad (35)$$

This result may be combined with equilibrium-constant expressions for complex formation with surfactant at concentration c_c

$$K_A = c'_a/(c_a c_c); \qquad K_B = c'_b/(c_b c_c) \qquad (36,37)$$

The result is

$$\alpha = ((K_A c_{as} c'_{bs}/(K_B c_{bs}))+c_{as})(b_o/a_o)/(c'_{bs}+c_{bs}) \qquad (38)$$

If the fraction of the total A and B which is complexed is small, the ratio of uncomplexed A to B in the foam is the same as that in the pool ($a_s/b_s=a_o/b_o$). Hence

$$\alpha = ((K_A a_o)/(K_B b_o)+c_{as}/c'_{bs})(b_o/a_o)/(1 + c_{bs}/c'_{bs}) \qquad (39)$$

If the enrichment is high, so that $b'_s > b_s$ and $b'_s > a_s$, then

$$\alpha = K_A/K_B \qquad (40)$$

The extent of liquid entrainment affects the validity of the assumption just made. If the entrainment is low, the enrichment is in fact high and Equation 40 is valid. As entrainment increases, the enrichment decreases, and α approaches unity.

In the ultimate selection among available surfactants, the values of the respective equilibrium constants will often be the determining factor. It is noted that the K's for chelate type interactions are usually much larger than those for similar numbers of unidentate interactions (M1).

Foamability. An even more essential consideration in the selection of surfactant is its ability to form mechanically suitable foams. As noted earlier a chelating surfactant will be restricted to concentrations below the total rare-earth concentration, in order to maximize the selectivity. For a given available surfactant, this restriction may prevent foam formation altogether, or it may restrict foaming to a single mode. Furthermore, the particular surfactant must not form an insoluble product with the rare-earth ions, since this will result in a precipitate flotation which markedly reduces internal reflux.

Proposed System

A highly effctive alternative way of obtaining the benefits of a chelating surfactant, which was adopted in this study, is to remove the function of specificity from the surfactant, introducing a separate chelating agent to complex selectively among rare-earth ions. Now the main requirement for the surfactant is that it be capable of attracting chelated ions into the surface. The surfactant concentration no longer is limited by the total rare-earth concentration, and may be chosen to yield optimum mechanical and chemical results.

From the standpoint of research flexibility this kind of system has other major advantages. First, a wide choice of chelating agents is available from among those which have shown large equilibrium constants and large selectivities. The chelating agent could be changed to obtain maximum separation for a given pair of ions without changing the surfactant. Second, by the same reasoning, the surfactant chemical could be changed without altering the specificity of chelation. while avoiding the use of any that would precipitate with the particular rare-earth chelate.

Chelating Agent. Ethylenediamine tetra acetic acid (EDTA) has been studied extensively as a chelating agent for many metal ions, and provides an average specificity over the entire range of rare-earth ions of $10^{0.4}$ (S11).

Equilibrium constants are shown in Table VI , along with the single-stage separation factor calculated from Equation 40 for the adjacent ions. The Nd/Ce separation is seen to be 4.27, and the factor for Sm/Ce to be 14.5.

The reaction between metal ion and EDTA is represented by

$$M^{n+} + H_2Y^{-2} = MY^{(n-4)} + 2H^+$$

at pH 4 to 5, and by

$$M^{n+} + HY^{-3} = MY^{(n-4)} + H^+$$

at pH 7 to 9 (L6). Since the tripositive rare-earth ion yields a negatively charged complex, a cationic surfactant is required to promote the separation.

The solubility of the EDTA/rare-earth chelate is adequate for a wide range of foaming tests; the chelate solubility for Sm^{+3} is 10.6 gm/l or 0.02M at 25° C (M6).

Surfactant. A cationic surfactant, Hyamine 1622, was selected to extract the negatively-charged rare-earth chelate. A quaternary ammonium salt, it has found application in other anionic extractions (J1,J2). In bulk solutions the Hyamine/ EDTA/ rare-earth combination showed no precipitation over the full range of conditions studied.

Terminology: Classes of Foaming

A wide difference in the observable foamabilities and foam behavior of different systems makes it necessary to classify the types of foaming which may be encountered in the range of foam-fractionation operations. The classification

Table VI. Stability constants for rare-earth/EDTA chelates and separation factors for adjacent species.

element	log of stability constant, log K	separation factor α (*)	separation factor α (**)
La	15.30	4.8	3.7
Ce	15.98	2.54	2.5
Pr	16.40	1.63	1.8
Nd	16.61	3.40	3.2
Sm	17.14	1.63	1.5
Eu	17.35	0.64	1.05
Gd	17.10	7.96	9.6
Dy	18.00	7.10	4.7
Er	18.85	2.96	3.1
Tm	19.32	0.438	0.55
Yb	18.88	8.94	1.9
Lu	19.83	----	----
Ho	-----	----	2.6
Dy	-----	----	1.6
Y	-----	----	1.5
Tb	-----	----	4.2
Gd	-----	----	---

(*) Bjerrum, Schwarzenbach, Aillen, Stability Constants Part I (Chem. Soc., London, 1957).

(**) J.E. Powell, F.H.Spedding, Chem. Eng. Prog. Sym. Ser., 55, no. 24, 101 (1959).

used here is based both on surface area and on specific liquid content (ratio of liquid volume to surface area, equal also to the lamellar half-thickness); it employs numerals to abbreviate a two-variable terminology involving "persistence" and uniformity which is essential although frequently overlooked. More than a single class of foaming is sometimes observed for a given system.

Class I foaming has the surface area constant with height (persistent), and the specific liquid content constant with height (uniform).

Class II foaming has the surface area constant with height (persistent), and the specific liquid content decreasing continuously with height (nonuniform).

Class III foaming has the surface area decreasing with height (transient), and the specific liquid content constant with height (uniform).

Class IV foaming has the surface area decreasing with height (transient), and the specific liquid content decreasing with height (nonuniform).

The behavior of each class is indicated schematically in Figure 6. The frontal dimension represents surface area, S, the receding dimension the specific liquid content, q, and the vertical dimension the height, h, in the foam. Class I foaming thus involves no change in height, while Class IV foaming involves the most marked change.

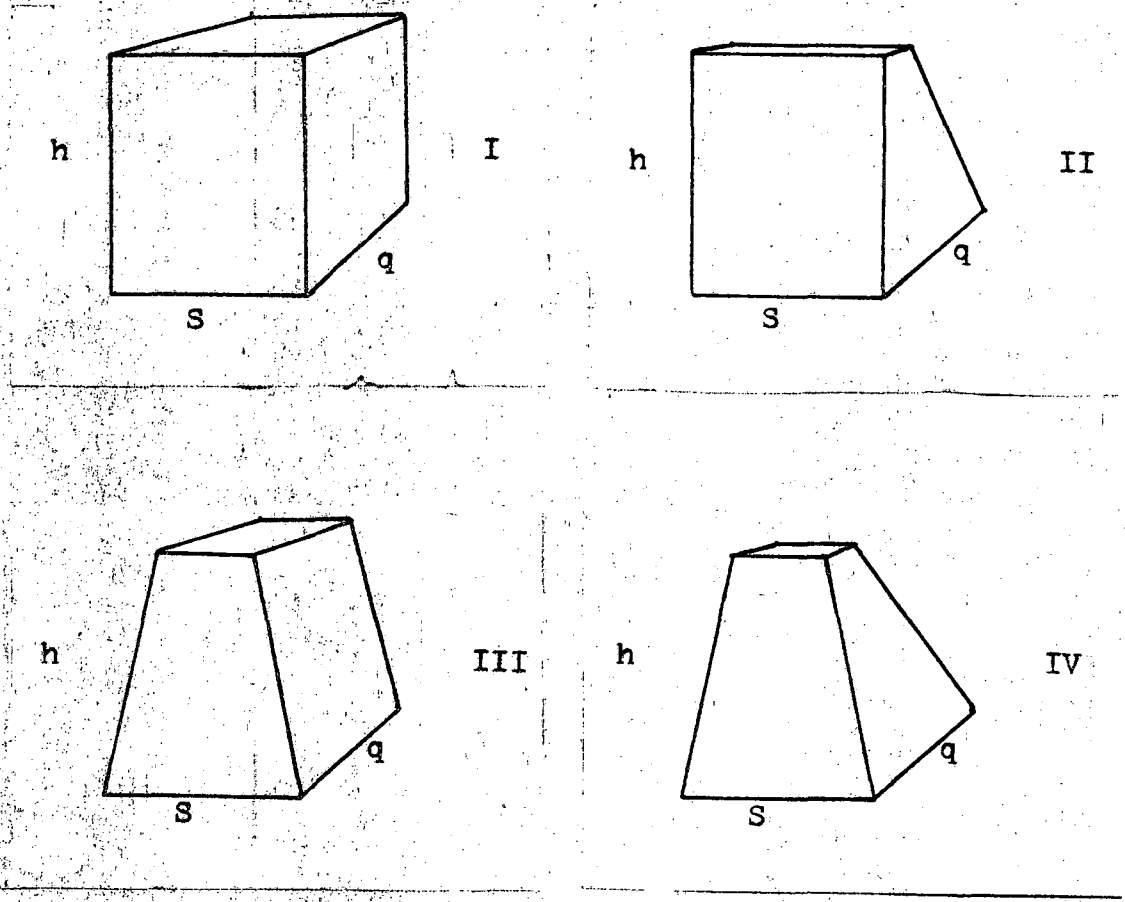

Figure 6. Schematic of surface S and specific liquid content q at different heights for the foaming classes.

The implication of this classification is seen most clearly in the behavior of the enrichment, E, expressed for one component or for a combination of several components; the separation factor, α ; and the effective extraction rate, M.

$$E = (\text{concentration in foam})/(\text{concentration in pool})$$

$$\alpha = \frac{(\text{concentration of A in foam})}{(\text{concentration of B in foam})} / \frac{(\text{concentration of A in pool})}{(\text{concentration of B in pool})}$$

$$M = (E-1)\cdot(\text{pool concentration})\cdot(S_v)$$

The variation of E, M, α , and S_v with height or $1/v_s$ is shown in Figure 7 for foaming in each class, based on a foam with the same structure for each class at zero height.

Enrichment in a class I foaming is invariant with height ($1/v_s$) because the concentration of the foam (the average of surface concentration and interstitial concentration weighted by the surface area and interstitial volume) is invariant with height. Enrichment continuously increases with height during a class II foaming because of continuous reduction of interstitial volume (and mass) and complete retention of the surface area (and mass).

Enrichment increases with height in both classes of transient foaming. In a class III foaming, part of the surface material rejected to the interstices will be retained in the foam and will not drain downward to the pool. Therefore, the actual rate of loss of total surface mass with height is

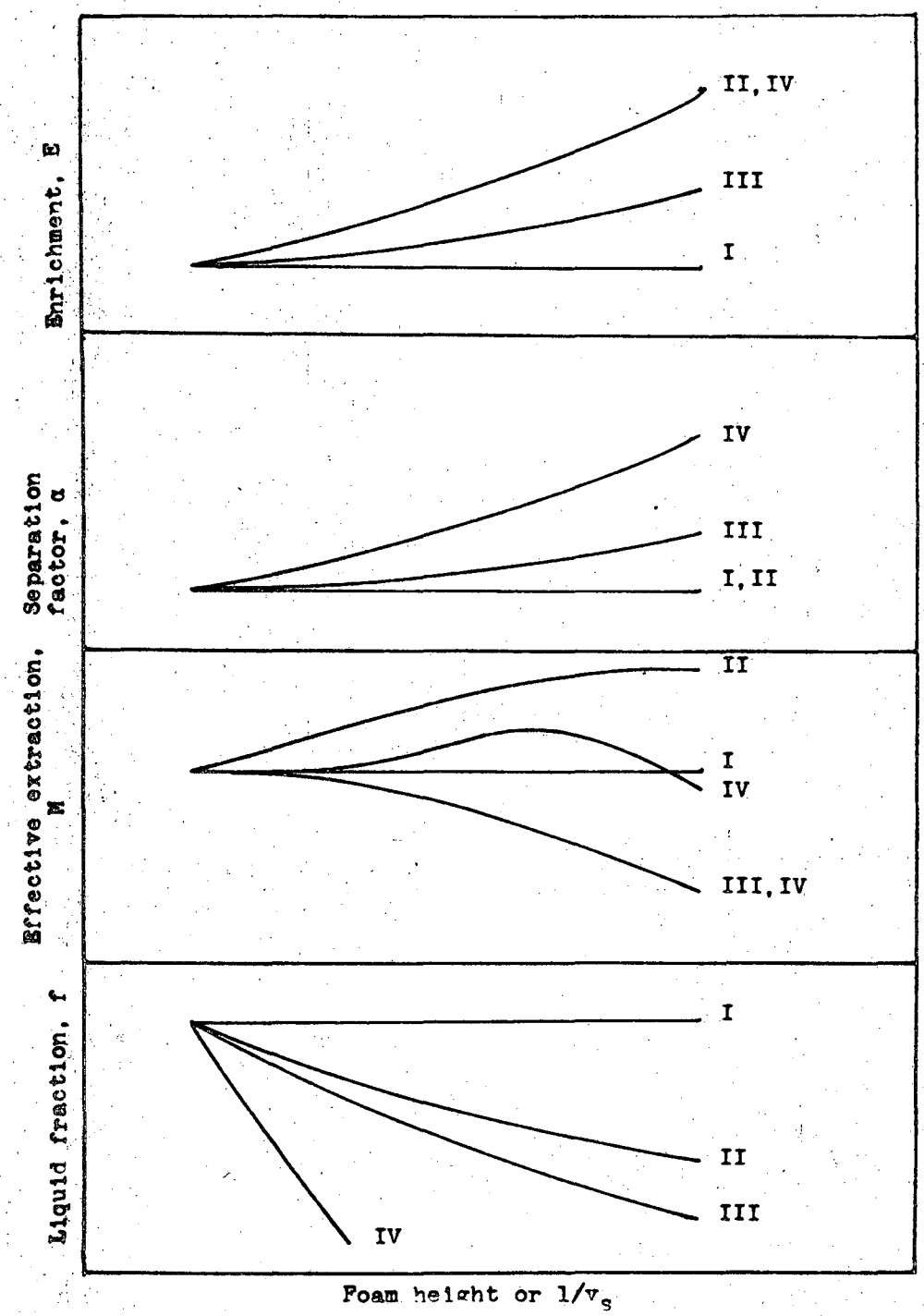

Figure 7. Effect of height ($1/v_s$) on separation performance for different foaming classes.

slower than the loss of total foam volume so that the enrichment must increase. In a class IV foaming, both the retention of rejected surface material and the loss of the specific liquid content, q, will contribute to increasing the enrichment.

No variation in the separation factor with height can occur in either class I or II foaming because the surface contacts only the pool-like liquid from which it was originally formed. Separation improvement with height may be obtained by supplying a reflux of condensed-foam product provided uncomplexed ions remain in the interstices to allow redistribution of the ions with the complexing agent.

Both class III and IV foaming should exhibit a separation factor which increases with height because of multiple contacting. The rejection of surface material to the interstices will change the distribution of complexed ions and increase the overall concentration in the intersticial liquid from the pool-liquid levels; and, thus, alter the equilibrium distribution of ions on the rising surfaces. A progressive displacement of uncomplexed ions will occur in the intersticial liquid with height, so that the greatest change in distribution of complexed ions will occur at an intermediate height.

The extraction rate in a class I foaming cannot change with height simply because the foam concentration and volume

is invariant. The extraction rate in a class II foam will increase in the range of heights in which the surface and intersticial mass are comparable and remain constant for heights where the surface mass predominates.

The extraction rate in class III and IV foaming will decrease with height because of loss of surface (and surface mass) if not all of the surface material rejected by coalescence is retained in the intersticial spaces. Initial increases in the extraction rate may be observed for class IV foaming as the result of more rapid loss of q (improving E) than of loss of surface.

The volume fraction of liquid in the foam is shown in Figure 7 as a function of height for the four foaming classes. In class I foaming f is constant. In class II foaming f decreases because of drainage, and in class III f decreases because of foam losses. In a class IV foaming f decreases because of drainage and foam losses.

In actual practice, all of the curves of Figure 7 will be preceded by a section of class II or class IV foaming (decreasing q with height) from the pool surface up to an intermediate height where the illustrated curves begin. Generally, E, α, and M all will start at zero values in this region because of the large amount of entrained liquid.

Experimental Effect of Gas Flowrate

In a fixed-height apparatus, for foaming at constant surfactant concentration, increasing the gas flowrate affects the class of foaming by reducing the time for coalescence and by increasing the liquid content (which protectively cushions the individual bubbles). Thus a low gas rate will favor class III and IV foaming, and a high gas rate will favor class I and II.

Foaming experiments for the extraction of the anionic surfactant Aerosol-22 at gas rates between 1.6 and 53 cm^3/min were performed from pool solutions maintained at 2.8×10^{-4} M and 11.8×10^{-4} M in surfactant by continuous feeding. The foam height was fixed at 6cm, and the pool volume was 60 cm^3. As shown in Table VII and Figure 8, increasing the gas rate from 1.6 to 53 cm^3/min caused a marked increase in the liquid content of the foam, and a suppression of the surfactant enrichment ratio. The maximum enrichments, at lowest gas flow rates, were 2.55 and 1.40 respectively, for solutions 2.8×10^{-4} and 11.8×10^{-4} M in surfactant. At 5 cm^3/min, the dilute solution gave an E around 2.0, while the more concentrated solution had E = 1.4.

Bubble coalescence, observed qualitatively, was seen to be excessive at the lowest flow rates but decreased to zero at the highest flowrates, as predicted. This variation from class III-IV foaming to class I-II foaming with increasing gas

Table VII. Foaming of Aerosol-22 solutions: effects of surfactant concentration and gas flowrate.

Aerosol feed$_4$ (Mx10^4)	gas rate, G (cm^3/min)	v_s (cm/sec)	Aerosol foam$_4$ (Mx10^4)	enrichment, E	foam liquid rate, S_V (cm^3/min)	foam liquid fraction, f
11.7	5.1	0.0168	16.4	1.40	0.26	0.0481
11.8	21.6	0.0713	11.8	1.00	2.02	0.0856
11.8	52.3	0.169	11.8	1.00	11.8	0.184
11.8	52.6	0.170	13.6	1.14	8.07	0.133
2.92	1.59	0.00525	7.50	2.56	0.07	0.0429
2.95	8.8	0.0293	5.02	1.70	0.58	0.0617
2.95	13.8	0.0456	4.14	1.40	0.86	0.0585
2.78	25.8	0.0852	3.62	1.30	2.26	0.0804
2.78	42.1	0.139	3.00	1.08	5.17	0.109

All experiments performed in a 6cm tall foaming column.

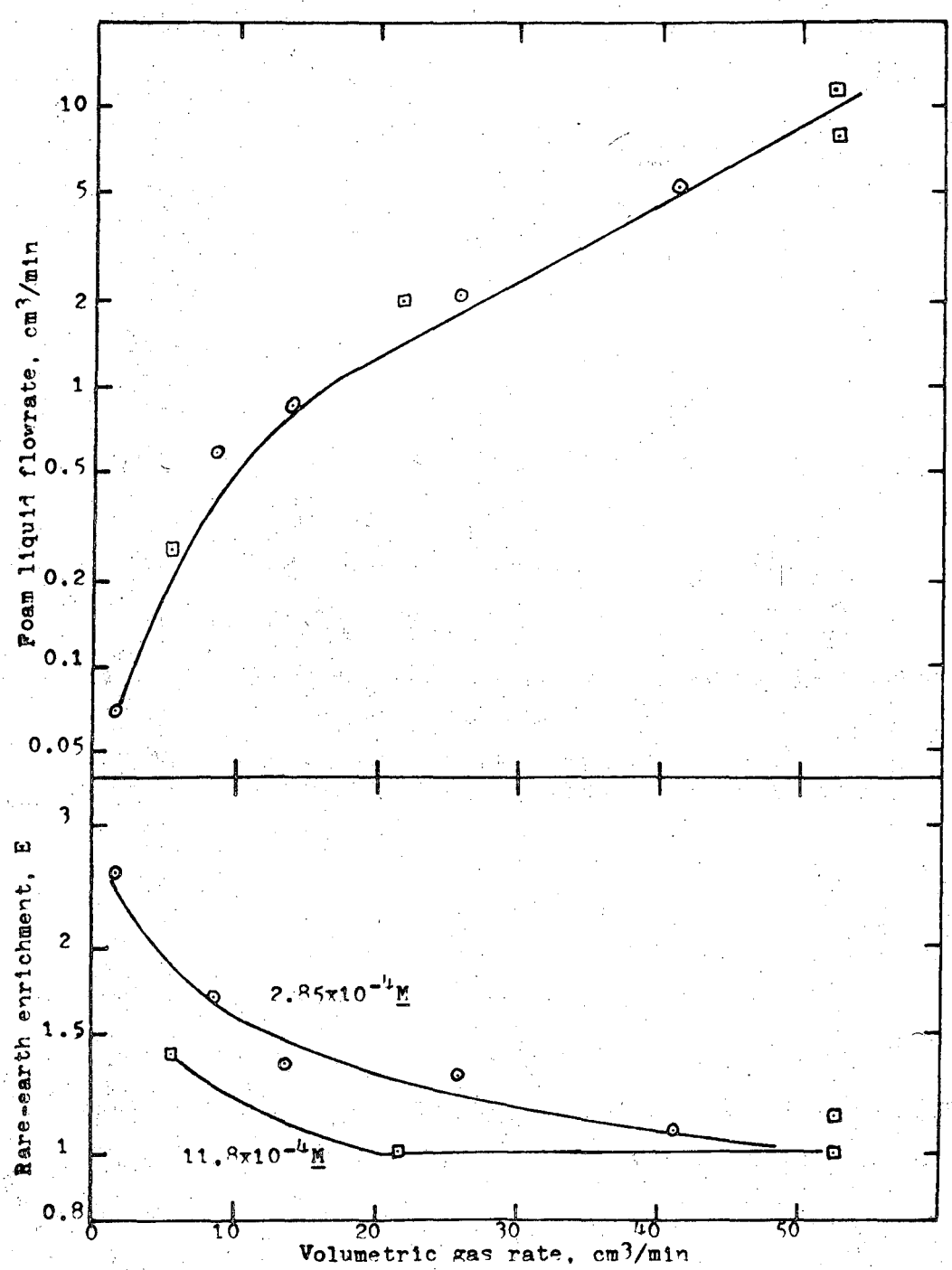

Figure 8. Effect of gas rate and concentration on Aerosol-22 separation in 6cm foam.

flow rate is also shown by the data for liquid entrainment, which may be compared with the schematic Figure 7.

Experimental data for foam liquid-fraction f are plotted against gas velocity v_s on logarithmic coordinates in Figure 9. For such plot, in class II foaming, the theoretical slope will be between 0.75 and 1.0 (H1, H2, L1, L2, L4, R5, R6). The experimental data observed have a slope of about 0.2 below 0.06 cm/sec and approach a slope of 0.71 above this value. Thus, indirectly, class III and IV foaming can be identified by the gross deviation from class II behavior at the low gas rates. Qualitatively, inclusion of the increasing bubble size (as observed at the foam exit at low gas velocities) would give higher fd^2 values (applicable in class I foaming) and would shift the transition point to class I-II foaming to about 0.1 cm/sec.

The effect of gas flow rate on the effective extraction rate (M, calculated from the smooth curves of Figure 8, is reported in Table VIII and Figure 10. Maxima in M at gas rates of 9 cm^3/min for the concentrated solutions and at 25 cm^3/min for the dilute solutions are the result of a balance between the increasing surface area (which increases M) and increasing liquid content (which decreases M).

The important consequence of this last result is that maximum extraction occurs in class III-IV foaming for higher bulk surfactant concentrations, but in the direction of class

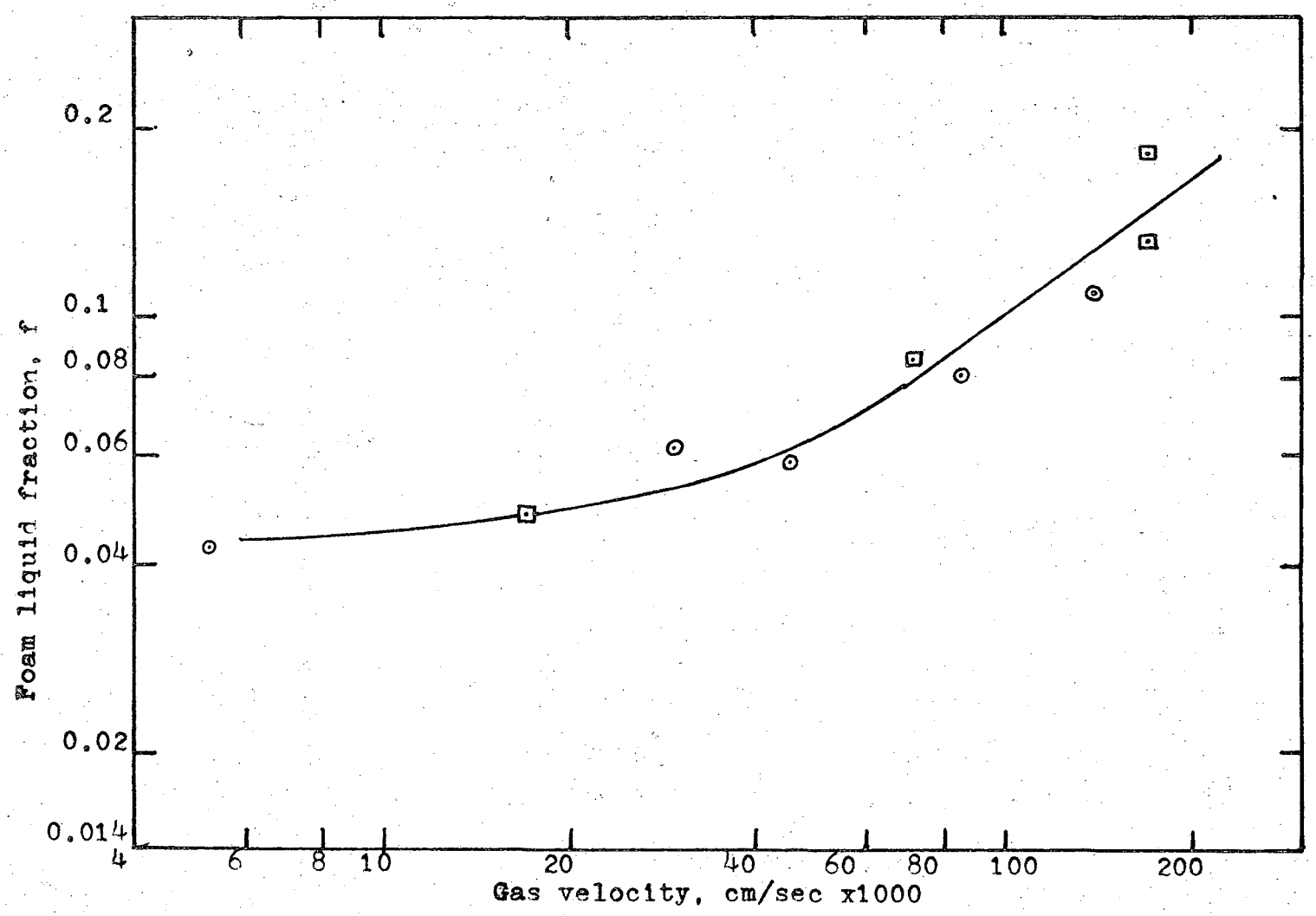

Figure 9. Effect of gas rate on foam liquid fraction; Aerosol-22 experiments.

Table VIII. Foaming of Aerosol-22 solutions: smoothed values of extraction rate at 6cm heights.

Aerosol feed (moles/cm^3)	gas rate (cm^3/min)	enrichment E-1	foam liquid rate, S_v (cm^3/min)	extraction rate (moles/min)
2.85×10^{-7}	2.0	1.35	0.075	2.88×10^{-8}
	4.0	1.04	0.145	4.25
	6.0	0.83	0.235	5.56
	8.0	0.67	0.365	6.95
	10.0	0.57	0.510	8.27
	15.0	0.42	0.900	10.7
	20.0	0.31	1.27	11.2
	25.0	0.23	1.73	11.3
	30.0	0.16	2.38	10.9
	35.0	0.12	3.25	11.1
	40.0	0.08	4.50	10.3
	42.5	0.06	5.25	8.95
	45.0	0.04	6.10	4.51
	50.0	0.00	8.40	0.00
11.8×10^{-7}	3.0	0.58	0.105	7.18
	4.0	0.50	0.145	8.55
	5.0	0.43	0.185	9.40
	6.0	0.38	0.235	10.5
	7.0	0.33	0.295	11.5
	8.0	0.28	0.365	12.1
	9.0	0.24	0.435	12.3
	10.0	0.20	0.510	12.1
	11.0	0.17	0.590	11.8
	12.0	0.15	0.670	11.9
	13.0	0.12	0.760	10.8
	14.0	0.10	0.850	10.0
	15.0	0.08	0.900	8.50
	16.0	0.06	0.990	6.95
	17.0	0.05	1.05	6.15
	18.0	0.04	1.12	5.31
	19.0	0.02	1.20	2.83
	20.0	0.01	1.27	1.53

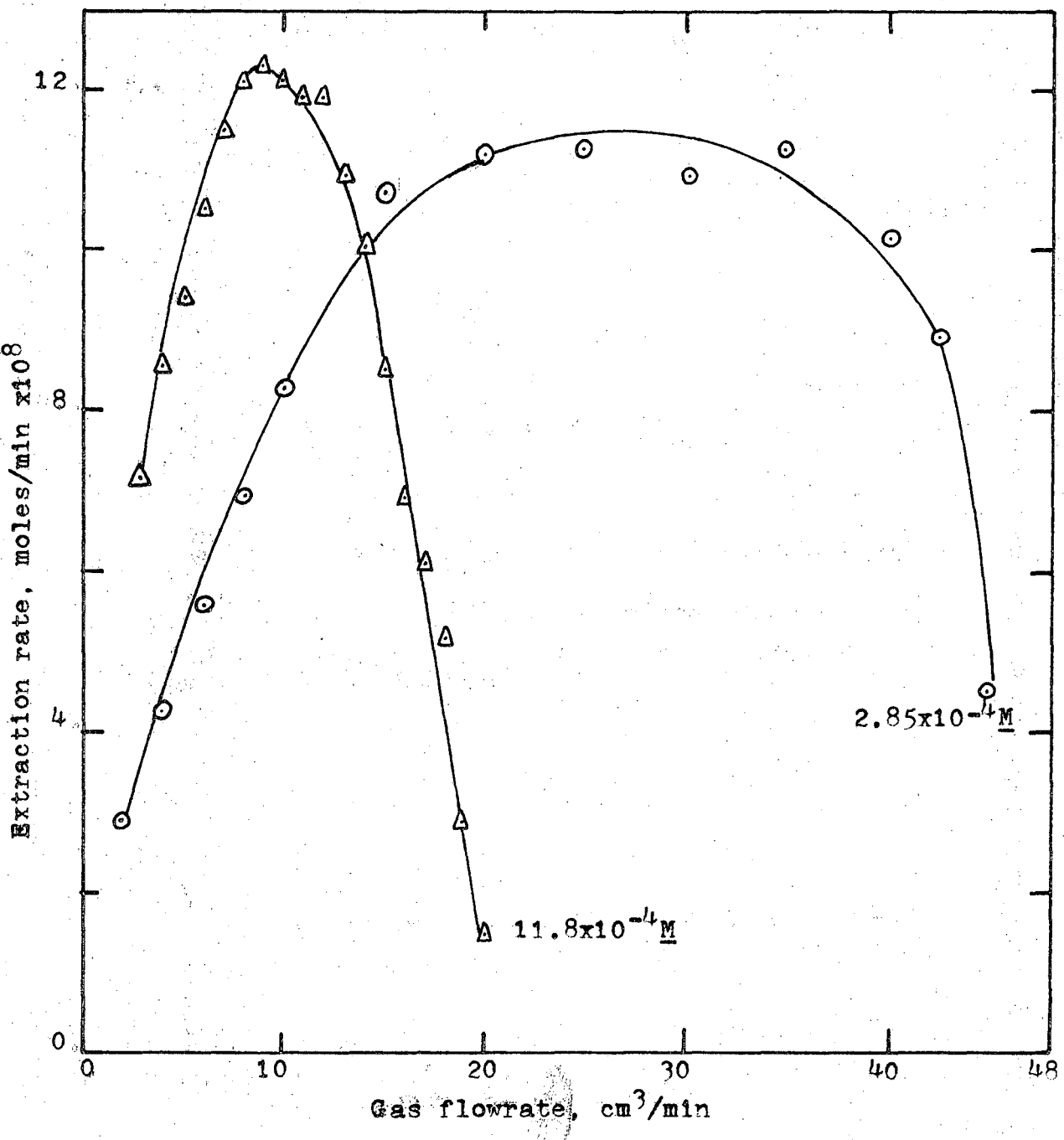

Figure 10. Effect of gas rate and concentration on Aerosol-22 extraction.

II foaming for lower surfactant concentrations. The general implication is that a system susceptible of foaming in either mode I-II (persistent) or modes III-IV (transient) may be separated to advantage in a transient mode. The greater enrichment observed with high extents of coalescence (at low gas rates) reinforces this conclusion.

As a corollary practical result, the gas rate to be selected for maximum effective extraction (or for a compromise between maximum effective extraction and maximum enrichment) will depend strongly on the concentration of the solution. As the concentration falls, in a batch extraction, the gas rate should be continuously increased; in a continuous extraction, operation in stages would be necessary, with the respective gas flow rates increasing from the solute-rich to the solute-lean end of the cascade.

RESULTS AND DISCUSSION (PART II): RARE-EARTH SEPARATIONS

Class of Foaming

Experimental Effects of Surfactant Concentration. Surfactant concentration is important to the class of foaming; increasing the concentration increases film elasticity and bulk viscosity so that a transient class of foaming becomes more persistent (although class I or II foaming may not be reached). The extent to which foaming becomes persistent depends on the nature of the surfactant and on the physical conditions. Increasing the surfactant concentration to a high value will reduce the film elasticity, and thus return the foaming to a more transient mode.

This increase in persistence of foaming was observed in experimental studies of variation in total liquid content at different heights of foaming, at different concentrations of Hyamine 1622 in the presence of EDTA/rare-earth chelates. As reported in Table IX and Figure 11, the constant-concentration contours tend steadily toward a limiting class II oblique or a limiting class I horizontal curve; the closest approach to persistent foaming occurred at the highest tested concentration of surfactant (10.4×10^{-4} M, or 0.5gm/l).

Bubble coalescence was considerable at every concentration level, and greatest at the lowest levels. Coalescence was so great below 0.1 gm/l of surfactant that the foam

Table IX. Foaming of Hyamine/EDTA/rare-earth solutions: effects of surfactant concentration and foam height on foam liquid content.**

run no.	Hyamine feed (gm/l)	Hyamine feed ($Mx10^4$)	foam liquid content ($cm^3/minx10^2$)	foam height (cm)	gas velocity (cm/min)
328	0.486	10.4	2.18	33.0	1.21
335	0.100	2.14	11.19	10.0	0.943
336			11.03	10.0	0.858
332			0.906	17.6	0.800
338			1.36	18.5	0.858
345			1.45	18.0	0.830
352			1.62	17.2	0.875
354			1.88	17.3	0.890
361			1.31	17.2	0.862
363			1.42	17.7	0.843
334			0.628	23.7	0.940
353			0.667	23.7	0.850
370			0.328	33.5	0.856
333			0.198	33.5	0.860
316*	0.090	2.00	27.7	6.0	0.860
340	0.050	1.07	5.07	10.0	0.858
339			0.537	18.0	0.825
343			0.491	18.0	0.863
348			0.364	18.0	0.850
358			0.215	18.0	0.958
317*	0.0450	0.967	30.0	6.0	0.860
341	0.0300	0.644	1.82	10.0	0.963
318*	0.0240	0.516	30.0	6.0	0.860
344	0.0200	0.430	1.35	10.0	0.821

* These values corrected to 50mm column from 25mm column. All other values are for 50mm column

** Various EDTA and rare-earth concentrations.

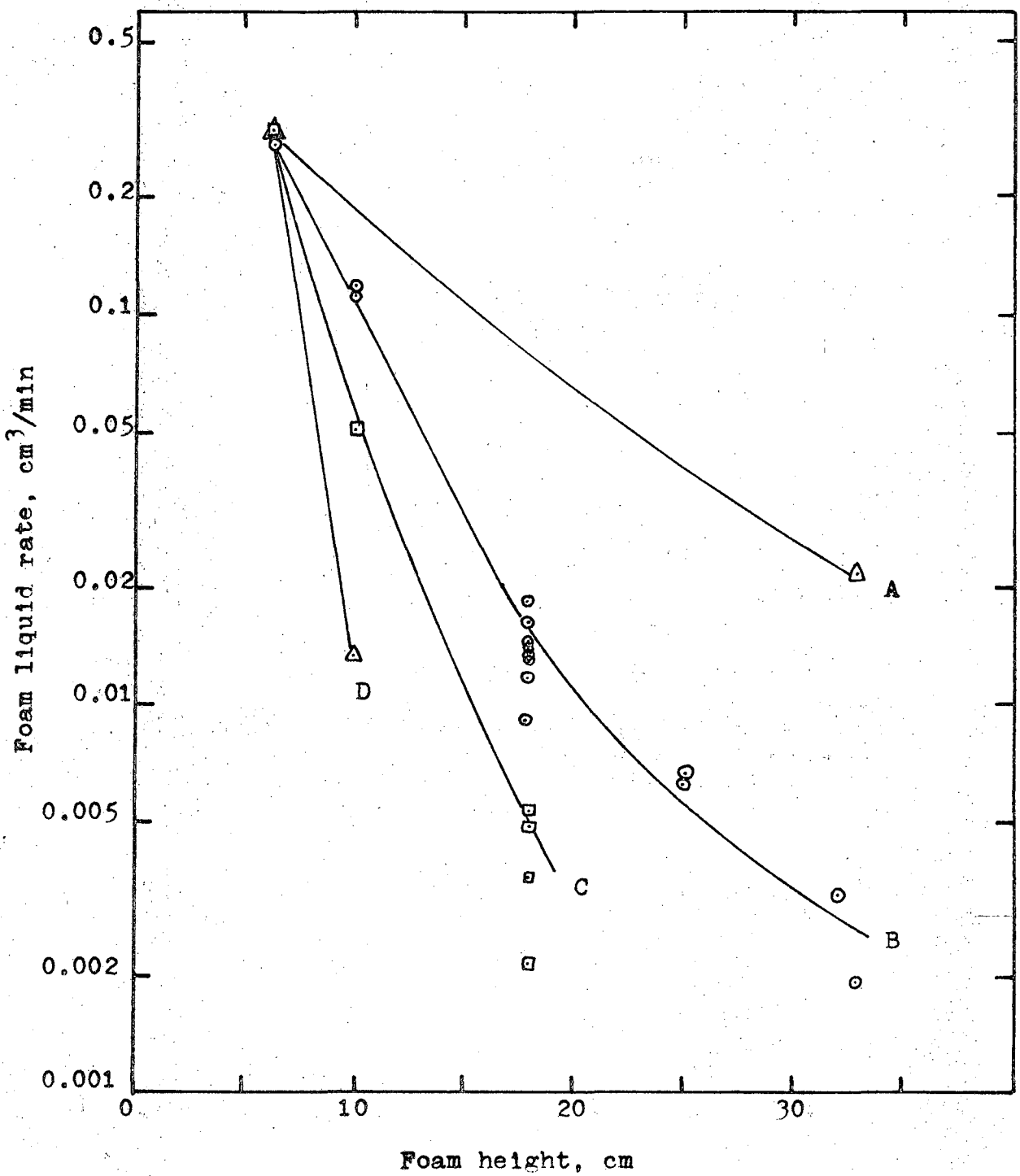

Figure 11. Effect of height and concentration on foam-liquid content of Hyamine foams. Surfactant at 0.5g/l (A), 0.1g/l (B), 0.05g/l (C), and 0.02g/l (D).

would not rise the entire 32-cm height of the apparatus during 5 hour run periods (curve C and D). The limiting height for foam collection decreased with decreasing concentration as indicated for curves B,C, and D of the figure.

The convergence of the constant concentration curves of Figure 11 to a common liquid content at low foam height indicates that the foam stability at such heights is due to the coalescence-resisting action of the bulk fluid, and to a concentration-independent drainage rate in this region of the column. The divergence of these curves at higher heights in the foam indicates that as the liquid drained downward from the foam, the concentration-dependent elasticity and viscosity became important in promoting the stability.

Identification of Foaming Class. The mode of transient foaming exhibited by Hyamine 1622 (0.100 gm/l, curve B) in the presence of EDTA/rare-earth chelates, was found to be class IV, by calculating the surface-area generation and specific liquid content from experimental data. The formulas used in the calculation were

$$S = G/(d/6) \tag{41}$$

and

$$S_v = Gq/(d/6) \tag{42}$$

Bubble diameters substituted into Equation 41 were taken from

the smoothed data reported in Table X and Figure 12 for a single foaming experiment from a solution 0.100 gm/l (2.14×10^{-4} M) in surfactant, 0.536×10^{-4} M in EDTA, and 3.90×10^{-4} M in total rare earth. The values of S_v substituted into Equation 42 were taken from the smoothed data of Figure 11 for foaming at 0.100 gm/l in surfactant.

The surface-generation rate reported in Figure 12 decreased from nearly 2000 cm^2/min at the pool surface to 595 cm^2/min at the 33-cm height. The variation with height was linear above a height of 10-cm, but decreased more rapidly in the 0 to 10-cm region. The shape of the individual bubbles changed from spherical below the 11-cm height to polyhedral above, which is consistent with the interpretation just given for the observed surfactant-independent drainage rates at (or below) 6 cm.

The specific liquid content reported in Table X and Figure 13 was proportional to the -2.2 power of the foam height. The thinnest lamella were 1.06×10^{-5} cm, only 1/50th as thick as the lamella near the pool surface.

The class IV foaming may apply only to foaming from solutions near 0.100 gm/l in surfactant and at a gas velocity of 0.86cm/min. More extensive bubble-size measurement versus height at different concentrations would be required for complete characterization.

Table X. Foam geometry (smoothed data)*

foam height (cm)	average bubble diameter, d (mm)	gas rate (cm^3/mim)	surface generation rate (cm^2/min)	foam liquid rate (cm^3/min)	specific liquid content (cm)
0.5	0.53 ±0.02	----	-----	----	----
2.5	----	18.2	16.3×10^{2}	----	----
5.0	----	18.2	13.5	0.36	26.7×10^{-5}
7.5	----	18.2	11.8	0.193	16.2
9.5	1.00 ±0.05	----	----	----	----
10.0	----	18.2	10.7	0.105	9.80
12.5	----	16.7	9.20	----	----
15.0	----	16.7	8.61	----	3.70
17.5	----	16.7	8.10	----	----
20.0	----	16.7	7.67	0.112	1.47
22.5	1.39 ±0.07	17.5	7.55	----	----
25.0	----	17.5	7.20	0.0055	0.77
27.5	----	16.9	6.62	----	----
30.0	----	16.9	6.30	0.00332	0.53
31.5	1.65 ±0.08	----	----	----	----

* Hyamine 0.100gm/l pH = 6.7
$SmCl_3$ 1.93×10^{-4}M
$CeCl_3$ 2.02×10^{-4}M

Surface generation from smoothed data of Figure 12.

Liquid content from smoothed data of Figure 11.

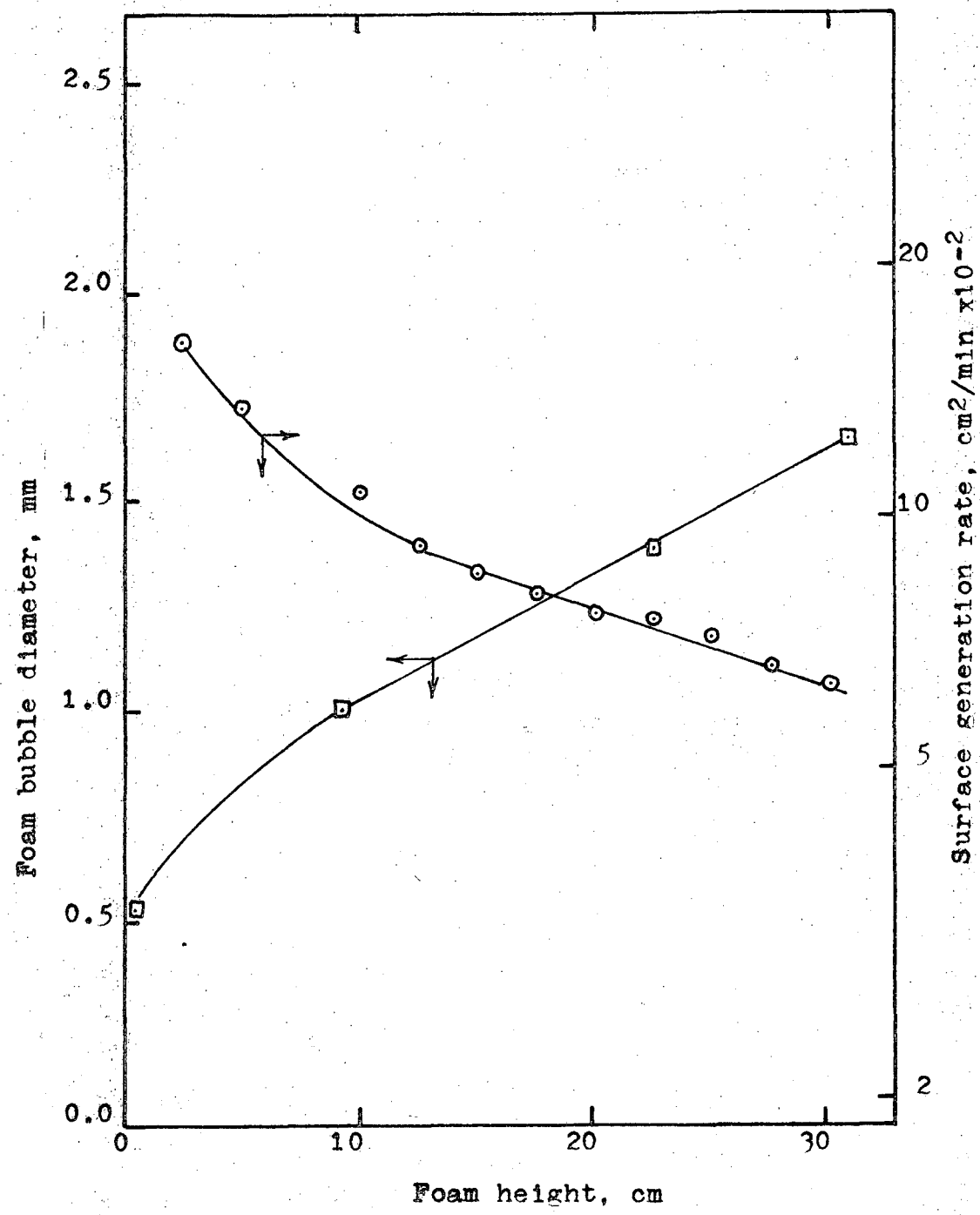

Figure 12. Effect of height on foam geometry in Hyamine (0.10g/l) foaming.

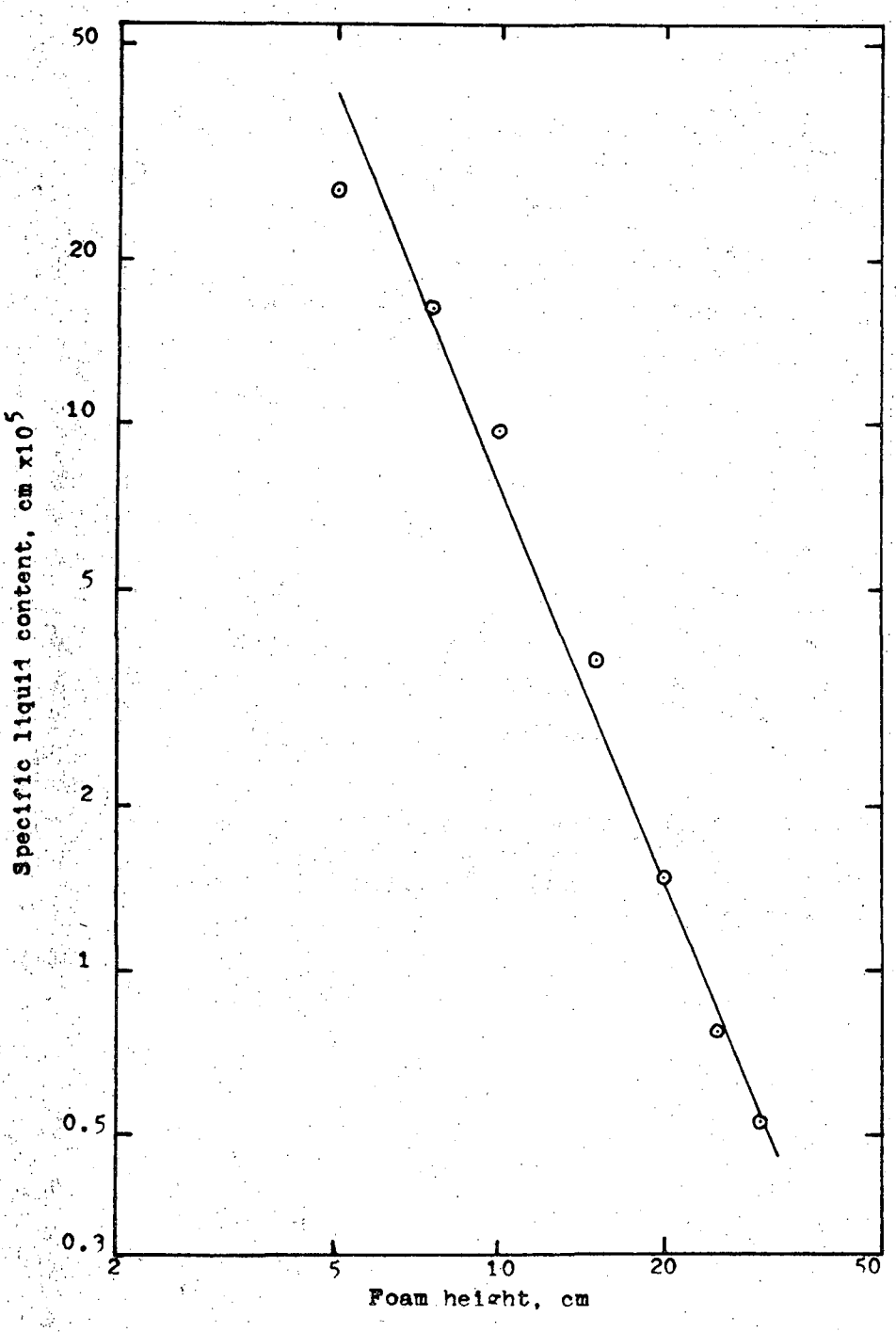

Figure 13. Effect of height on specific liquid content of Hyamine (0.10g/l) foam.

For want of bubble-size data, the calculation made at 0.100 gm/l in surfactant cannot be repeated for the lower concentrations. It would be difficult to measure bubble sizes at concentrations below 0.05 gm/l because of excessive coalescence, channeling, and gapping.

Effect of Column Height

The effect of height on rare-earth enrichment, separation factors, and extraction rates in a class IV foaming was examined for feed solutions containing 0.54×10^{-4} M EDTA, 4.8×10^{-4} M Nd^{+3}, 5.03×10^{-4} M Ce^{+3}, and 0.100 gm/l (2.14×10^{-4} M) Hyamine 1622, and is reported in Table XI and as curve E in Figure 14 and 15. Experiments at a lower rare-earth loading of 2.02×10^{-4} M Ce^{+3} and 1.93×10^{-4} M Nd^{+3} are also reported (curve F).

As expected in class IV foaming, the enrichment increased continuously with height, reaching 1.99 at 33cm for the high rare-earth loading and 5.31 at 24 cm for the low rare-earth loading.

The extraction rate M reported in Table XI and Figure 15 did not quite vary with height in the expected manner. Instead of reaching a maximum at an intermediate height and then decreasing, the extraction rate at the high rare-earth loading increased from zero at 10 cm to a value of 1.90×10^{-9} moles/min which remained constant for heights greater than 20cm (up to the maximum height measured, 33cm). The

Table XI. Effect of foam height and rare-earth loading on separation performance.

run no.	pH	feed $CeCl_3$ ($Mx10^4$)	feed $NdCl_3$ ($Mx10^4$)	foam height (cm)	enrichment, E	separation factor,	foam liquid rate (cm^3/min)	effective extraction rate (moles/min $x10^9$)	surface generation rate (cm^2/min $x10^{-2}$)	adsorption density (mole/cm^2 $x10^{11}$)
345	6.75	2.02	1.93	17.5	2.96	1.81	0.0145	11.2	7.10	1.58
337	6.70	2.02	1.93	24.0	5.31	----	0.0026*	10.7	5.90	1.82
335	6.50	5.03	4.80	10.0	0.96	1.15	0.1119	----	----	----
332	6.56	5.03	4.80	17.0	1.19	1.80	0.00906	1.69	8.30	0.204
334	6.48	5.03	4.80	24.0	1.31	1.89	0.00628	1.91	7.10	0.261
333	6.55	5.03	4.80	33.0	1.99	1.90	0.00198	1.92	5.90	0.326

Surface generation rate from Figure 12.

* Leak in foam-exit section makes this lower than actual; value used in calculation of adsorption density and effective extraction rate was 0.0063 cm^3/min from Figure 11.

5-Nov-75

Uncl (UCRL-Trans--1522) Studies for dimensioning a heavy ion linear accelerator of the Wideroe type (dimensioning of the four Wideroe sections of the UNILAC accelerator). KASPAR, K. (GESELLSCHAFT FUER SCHWERIONENFORSCHUNG M.B.H., DARMSTADT (F.R. GERMANY)). Oct 1973. Translation of GSI--73-10. 92p. Dep. NTIS $7.75.

20G particle accelerators; translations
MN-28 P NSA;ERA
EDB-430100;

Ekerdt

LBL 19525

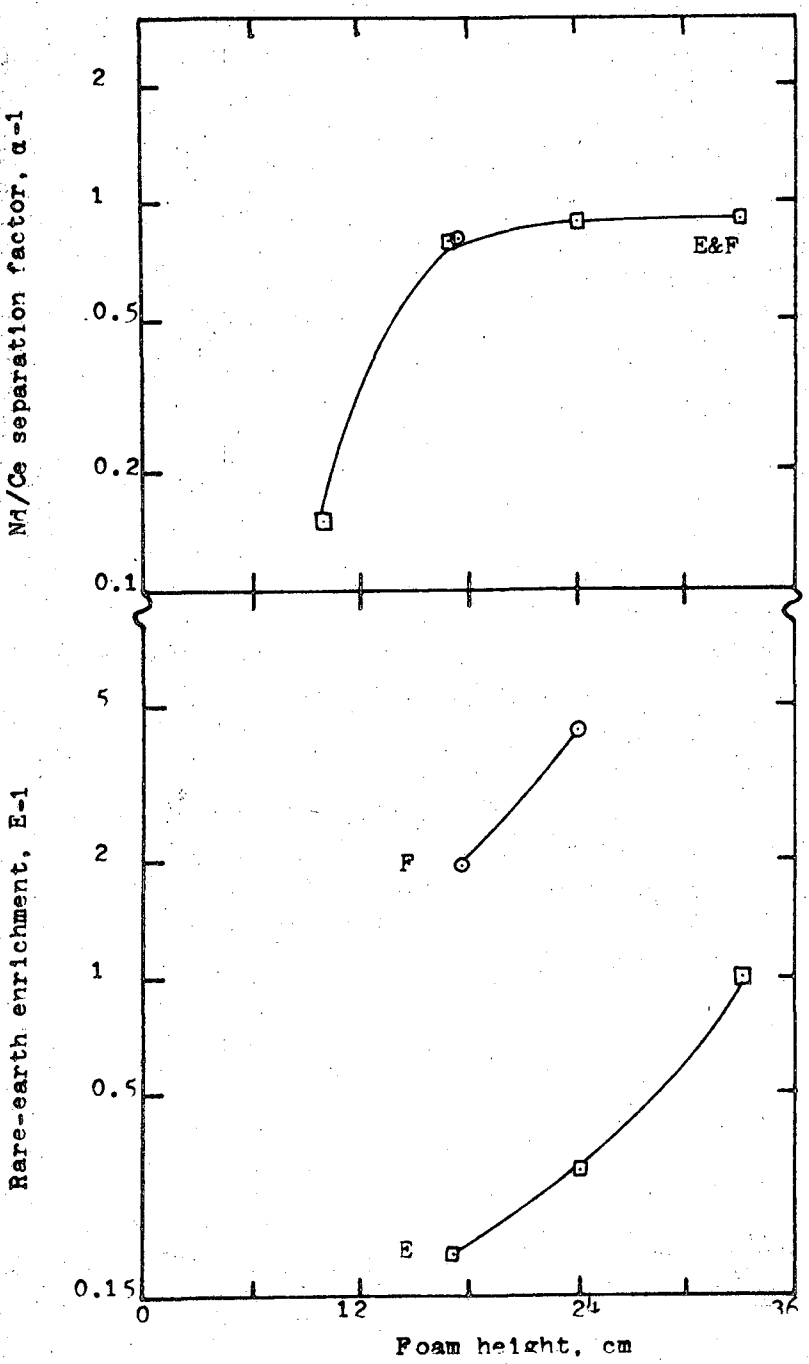

Figure 14. Effect of height and rare-earth loading (3.9×10^{-4} M, F; 9.8×10^{-4} M, E) on Nd/Ce separation and total enrichment.

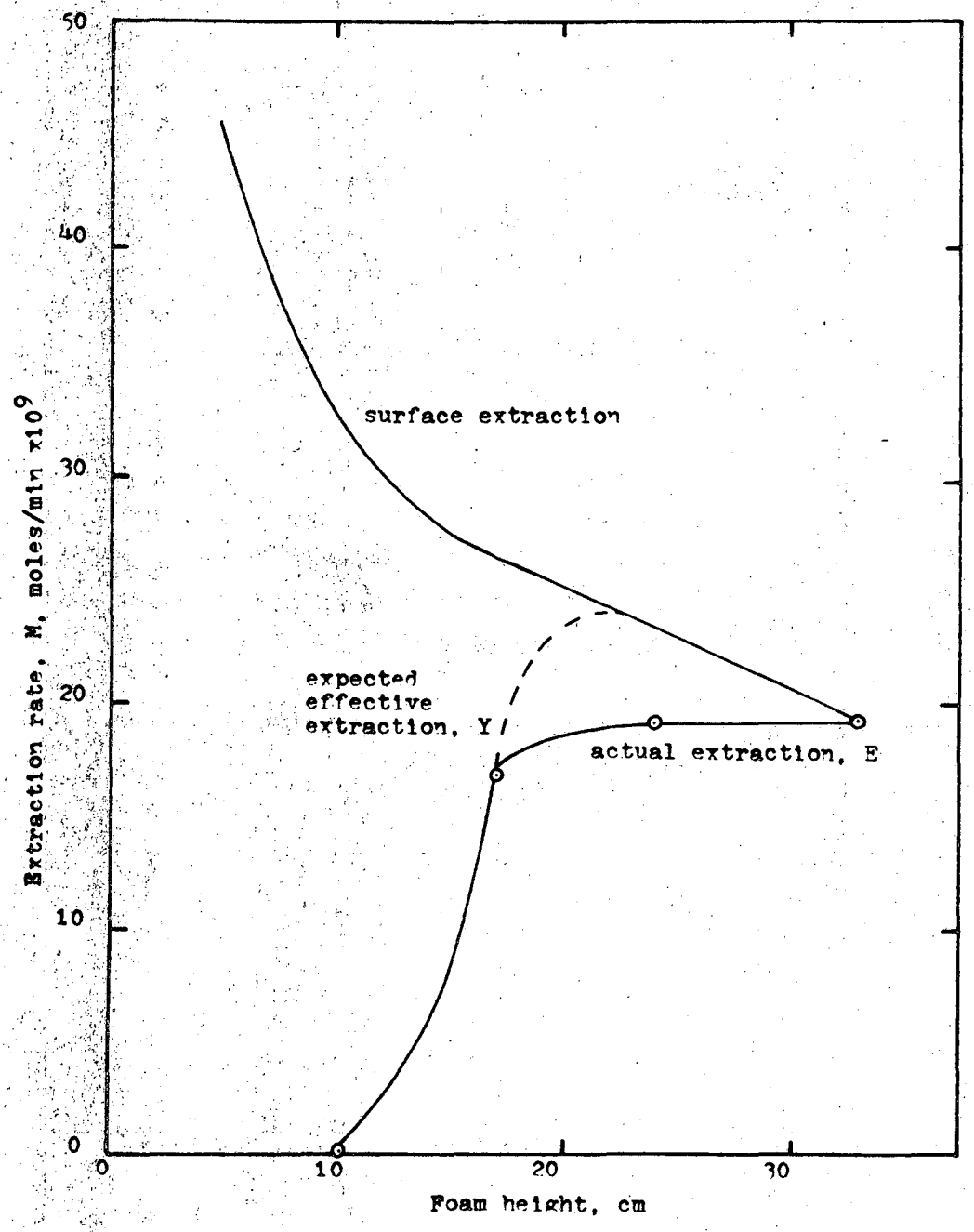

Figure 15. Effect of height on extraction rate of rare earth for high total loading (9.8×10^{-4} M).

extraction rate at the low rare-earth loading was constant at 10.9×10^{-9} moles/min above 17cm (up to the highest measured, 24cm). The expected kind of variation of mass extraction with foaming height is shown by the dashed curve of Figure 15. This curve parallels the surface-excess curve (back-calculated, assuming the adsorption density is constant at the actual foam value measured for 32cm) for tall foam heights, but drops to zero for short foam heights where the bulk negative "excess" of rare earth in the interstitial liquid balances the positive excess on the foam surfaces.

Constancy of total rare-earth product, while the surface area is decreasing, may be explained in one or more of three ways. First, the coalescence of foam bubbles may not result in a loss of surface material to the intersiicial liquid, but instead may involve surface rearrangement to a greater packing density. This possibility occurs because the surface coverages are many times greater than molecular areas: 8150 $Å^2$/rare-earth ion at 17cm and 5090 $Å^2$/rare-earth ion at 33cm for high loading, and 925 $Å^2$/rare-earth ion at 17cm and 1060 $Å^2$/rare-earth ion at 24cm for low loading. (These high coverages are not uncommon, and are comparable to those observed in surface-pressure studies for quaternary ammonium salts reported by Davies and Rideal (D3).)

A second explanation is that coalescence may accelarate a replacement in the new surface of uncombined surfactant by

surfactant combined with rare-earth chelates. This exchange does not alter the surface density of total adsorbed surfactant, but does result in a greater density of combined surfactant. Since only the rare-earth content of the foam, and not its EDTA content, was measured, such exchange would be seen only as a constant rare-earth mass with height.

Neither the total mass conservation or the rare-earth mass conservation would result in an internal reflux, and both would therefore yield a constant separation factor with height. This constancy of α at 1.90 for both loadings is consistent with the validity of either of these two interpretations.

A third explanation is that coalescence results in the rejection of both combined and uncombined surfactant from the newly formed surface, and that no rearrangement or change of density of surface material occurs. The observed constancy of mass with height is the result of retention of the rejected surface material in the foam interstices. This explanation is not entirely acceptable, because continuing drainage of intersticial liquid must carry some of this rejected material downward through the foam. For instance, between 17 and 33cm the 25% loss of surface (830 to 590 cm^2/min) by this mechanism would reject 25% of the surface mass to the intersticial liquid. Only a fraction of this mass could be retained, however, because there is

a concurrent 80% reduction in the specific liquid content from 2.0×10^{-5} to 0.44×10^{-5} cm.

Further experimental study might be useful to determine which of the first two mechanisms was acting. A foaming extraction of rare-earth ions by an anionic-chelating surfactant would be susceptible only to the surface exchange. Surface repacking and density increases would not be likely because the surface coverages of 20 to 30 $Å^2$/ion typical of anionic surfactants are on the order of the molecular dimensions.

Extraction by an anionic surfactant would also achieve greater enrichments as a result of the smaller surface coverage and enable efficient foaming at higher loadings of rare earth.

The constant Nd/Ce separation factor of 1.90, obtained above the 17cm level at both rare-earth loadings, was lower than expected. The limiting value of α should be the same as the ratio of chelated Nd to Ce (3.75:1) as calculated from the equilibrium constants. The reason for a low α (in spite of continuously increasing enrichment) was taken as evidence of nonspecific coadsorption of uncomplexed rare-earth ions in a triple layer or extended double layer. This coadsorption of uncomplexed rare-earth ions is consistent with the constancy of α with height in the foam because the coadsorbed ions would be retained with the chelated rare earths.

Future experiments could avoid this coadsorption by foaming uncomplexed rare-earth ions with an anionic surfactant in the presence of a chelating agent which forms uncharged complexes with the rare earths.

Effect of Rare-Earth Loading

The large difference in extraction rates reported in Table XII between the high and low rare-earth loadings is the probable result of a pH effect and a solubilizing effect. The pH change between the two loadings (pH=6.5 at high loading and 6.7 at low loading) is sufficient to cause a nearly four-fold increase in extraction. (As seen in the constant rare-earth concentration experiments 338 and 347 of Table of the section on the effects of pH, a pH change from 6.5 to 6.7 causes E-1 (andM) to increase by a factor of 4.)

The observed extraction increase from 1.9 to 10.9×10^{-9} moles/min between the high and low loadings is greater than a five-fold change, however; the additional difference may be due to the effect of excess uncomplexed rare earth in solubilizing the chelated rare earth and preventing its surface adsorption. This solubilization would be greater in the high loading (greater reduction of M) where the excess of uncomplexed rare earth is greater by a factor of 3.

Effect of Surfactant Concentration

The effect of the foaming stability on rare-earth enrichment, separation, and extraction rate was examined in

experiments in which surfactant concentration was the independent variable, as reported in Table XII and Figure 16. The feed solutions for these experiments were 2.14×10^{-4} M or less in surfactant, 0.55×10^{-4} M in EDTA, 2.02×10^{-4} M in Ce^{+3}, and 1.89×10^{-4} M in Nd^{+3}.

The total rare-earth enrichment ratio was suppressed in both 10 and 17cm foams, as the concentration of surfactant increased and forced the foaming toward a persistent mode. The suppression of enrichment ratio E in a 10cm foam was from 1.26 to 1.06 for the surfactant range of 0.044×10^{-4} M to 2.14×10^{-4} M.

Increasing the surfactant concentration could have suppressed the enrichment ratio in either of two ways. First, a high surfactant concentration should tend to favor surface-adsorption of the free surfactant over that of surfactant combined with rare-earth chelates. Second, the specific liquid content of the foam should be raised by the effects of larger surfactant concentrations in increasing the bulk and surface viscosities. Competition between the foam surfaces and homogeneously dispersed micelles is not likely since the critical concentration for micelle formation (1 g/l), determined from the break in the Hyamine surface-tension/concentration curve, was not exceeded in any experiment (R7).

The separation factor in the 10cm foam was constant at 1.35, up to a surfactant concentration of 0.05g/l. It then decreased, reaching 1.09 for a concentration of 0.100g/l.

Table XII. Effect of surfactant concentration on separation performance.*

run no.	Hyamine feed ($Mx10^{4}$)	foam height (cm)	enrichment, E	separation factor, α	foam liquid rate (cm^3/min) $x10^2$
341	0.644	10.0	1.26 ±5%	1.31 ±7%	1.82
340	1.08	10.0	1.17 ±1%	1.36 ±8%	5.07
336	2.13	10.0	1.06 ±4%	1.09 ±8%	11.02
339	1.11	17.5	4.84 ±4%	1.84 ±9%	0.537
338	2.16	18.5	1.54 ±5%	----	1.36
337	2.12	24.0	5.31 ±2%	----	0.256**

* $CeCl_3$ $2.02x10^{-4}M$
$NdCl_3$ $1.91x10^{-4}M$
EDTA $0.55x10^{-4}M$
gas rate 0.86 cm/min

** Leak in foam-exit section makes this lower than actual

UCRL-19525

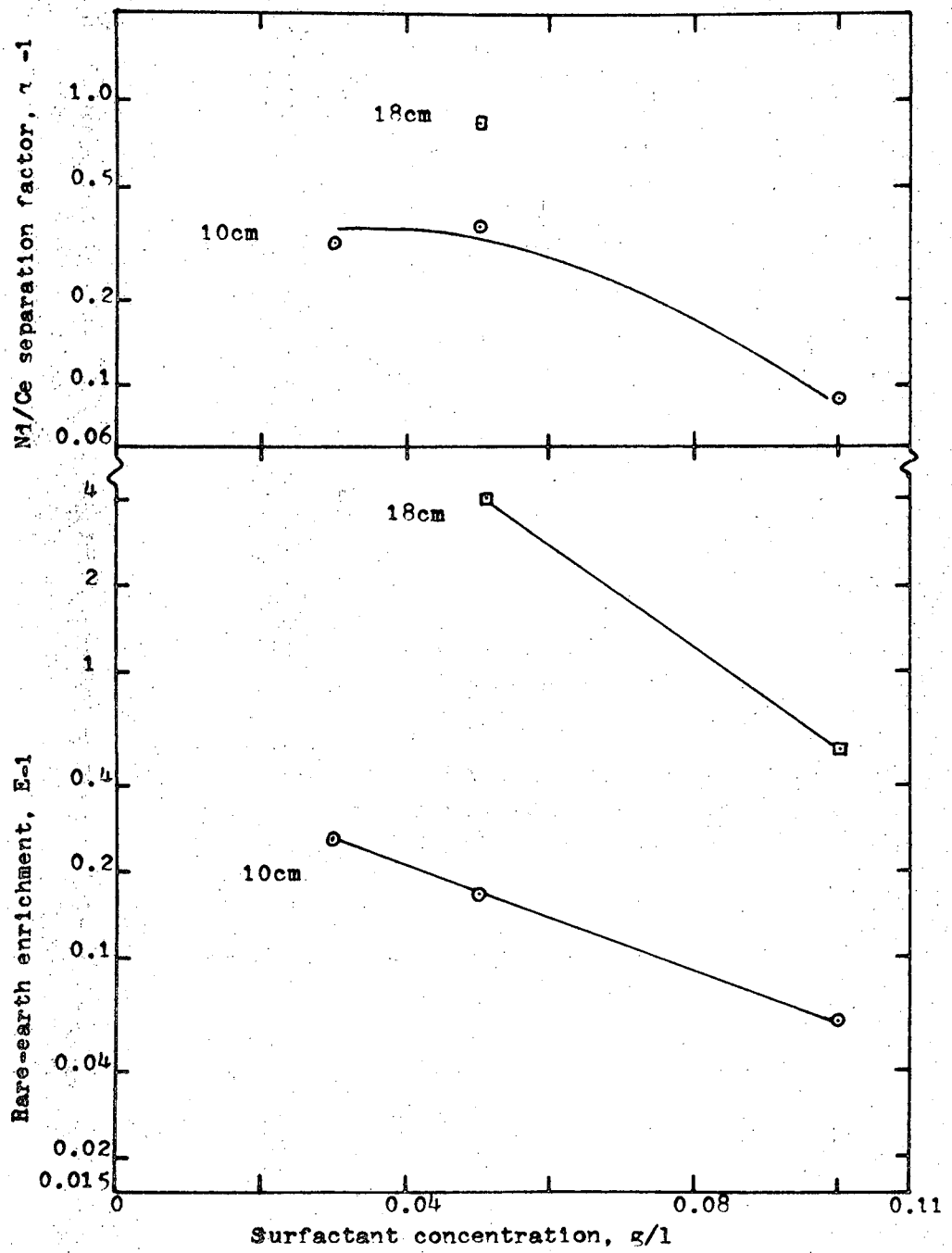

Figure 16. Effect of surfactant concentration on rare-earth enrichment and Nd/Ce separation.

The constancy of α in the low-surfactant range indicates that, here, increments of surfactant increase the total surface more than they increase the specific liquid content. The decrease in the separation factor in the range above 0.05 gm/l is viewed as being due to a greater increase in q, along with increased competition for surface sites as discussed in the preceding paragraph.

The extraction rate (calculated from Figure 11 and Figure 16, and reported in Table XIII and Figure 17) decreased continuously as the concentration of surfactant increased above 0.05 gm/l in both 10 and 17cm foams. The reasons for this general decrease in extraction rate were discussed earlier in this section.

However, extraction rate for 10cm foaming at low concentrations (below 0.05 gm/l) increased to a maximum as a result of the balance between increasing surface area and increasing specific liquid content. Foaming below 0.05 gm/l, observed visually, exhibited gapping and channeling in the foam column.

The most important observation to be made from these studies is that the best separation, enrichment and extraction rate (provided no gapping or channeling occurs) are obtained for the most transient foaming. Increases in surfactant concentration promote greater stability and wetness, and thus decrease the effectiveness of separation.

Table XIII. Effect of surfactant concentration on extraction rate (smoothed data).*

foam height (cm)	Hyamine feed (gm/l)	total rare-earth feed ($Mx10^4$)	foam liquid rate ($cm^3/minx10^2$)	enrich-ment, E-1	effective extraction rate (moles/min) $x10^9$
18.0	0.051	3.91	0.537	3.84	8.04
	0.060		0.640	2.75	6.87
	0.070		0.800	1.81	5.66
	0.080		0.970	1.20	4.56
	0.090		1.20	0.80	3.76
	0.100		1.36	0.53	2.82
10.0	0.03	3.91	2.15	0.260	2.18
	0.04		3.35	0.210	2.75
	0.05		5.20	0.170	3.36
	0.06		6.00	0.135	3.17
	0.07		7.00	0.110	3.01
	0.08		8.00	0.089	2.78
	0.09		9.40	0.073	2.68
	0.10		10.00	0.060	2.35

* Data based on Figure 11 and Figure 14.

UCRL-19525

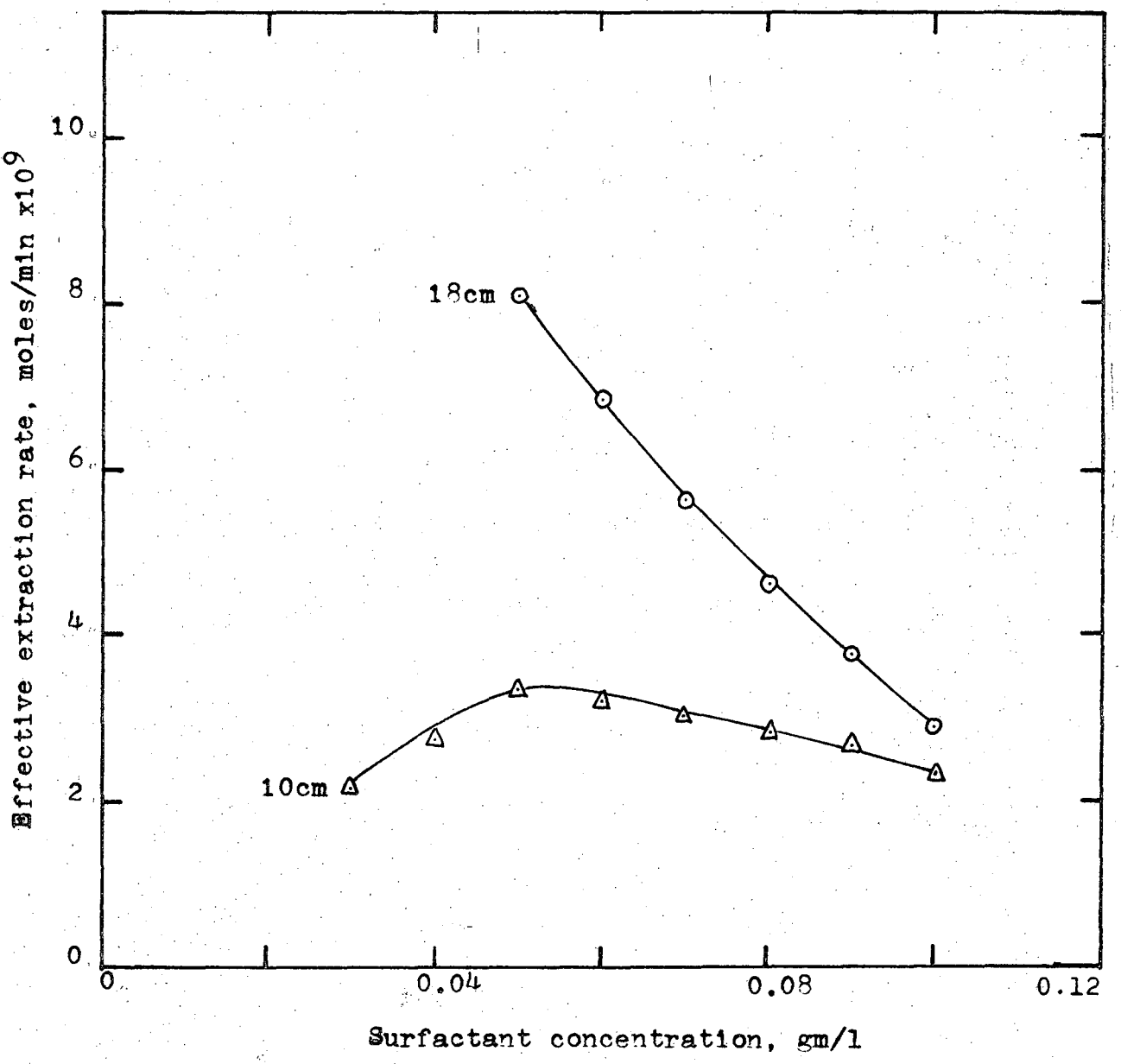

Figure 17. Effect of surfactant concentration on rare-earth extraction rate.

A corollary observation is that the most effective batch extraction of rare earths will be achieved by maintaining the surfactant concentration as low as possible during the operation. This might be achieved by repeating the two steps of (1) surfactant addition and (2) foaming until the desired level of depletion is obtained.

Effect of the Complexing Agent

The chelating agent, EDTA, was selected in order to obtain large separation factors between the individual rare-earth ions. The sole restriction on the EDTA seemed to be that its concentration be less than the total rare-earth concentration, so that interionic specificity could be observed. It was decided to test this premise experimentally by increasing the EDTA concentration from nil to a value in excess of the total rare-earth concentration. The results of this experimentation are reported in Table XIV and Figure 18.

Synergistic Behavior in Foaming. An important observation to be drawn from these data is that both free surfactant and combined surfactant must be present in order to produce foam, acting therefore in a synergistic relationship. The molar ratios of EDTA to surfactant in experiments 346 and 347 were 4.3:1 and 2.52:1, and in neither case was any foam formed. In experiment 346 enough excess EDTA was present to complex the surfactant completely and thus to prevent foaming. In experiment 347,

Table XIV. Effect of EDTA concentration on separation performance.

run no.	pH	feed Hyamine ($Mx10^4$)	feed EDTA ($Mx10^4$)	foam liquid rate (cm^3/min) x10^2	enrichment, E	effective extraction rate (moles/min) x10^9	separation factor, α	theoretical ratio of Nd/Ce on surface	semi-theoretical separation factor, α_t
325*	5.98	2.12	none	----	----	----	----	----	----
371*	6.70	2.14	none	----	----	----	----	----	----
355	6.71	2.14	0.174	1.96	1.16±5%	1.24	1.30±15%	4.10	1.43
379	6.68	2.16	0.404	1.85	2.07±5%	7.80	1.87±10%	3.54	2.32
345	6.75	2.09	0.564	1.45	2.96±2%	11.2	1.89± 8%	3.55	2.69
363**	6.70	2.18	1.26	1.42	5.78±1%	26.8	1.81± 3%	2.60	2.32
346*	6.71	1.03	4.44	----	----	----	----	----	----
347*	6.72	1.26	3.17	----	----	----	----	----	----

Theoretical surface ratio calculated from equilibrium constants.

Theoretical separation factor from theoretical surface ratio and experimental enrichment.

* No foam formed.
** White precipitat observed in condensed foam sample.

UCRL-19525

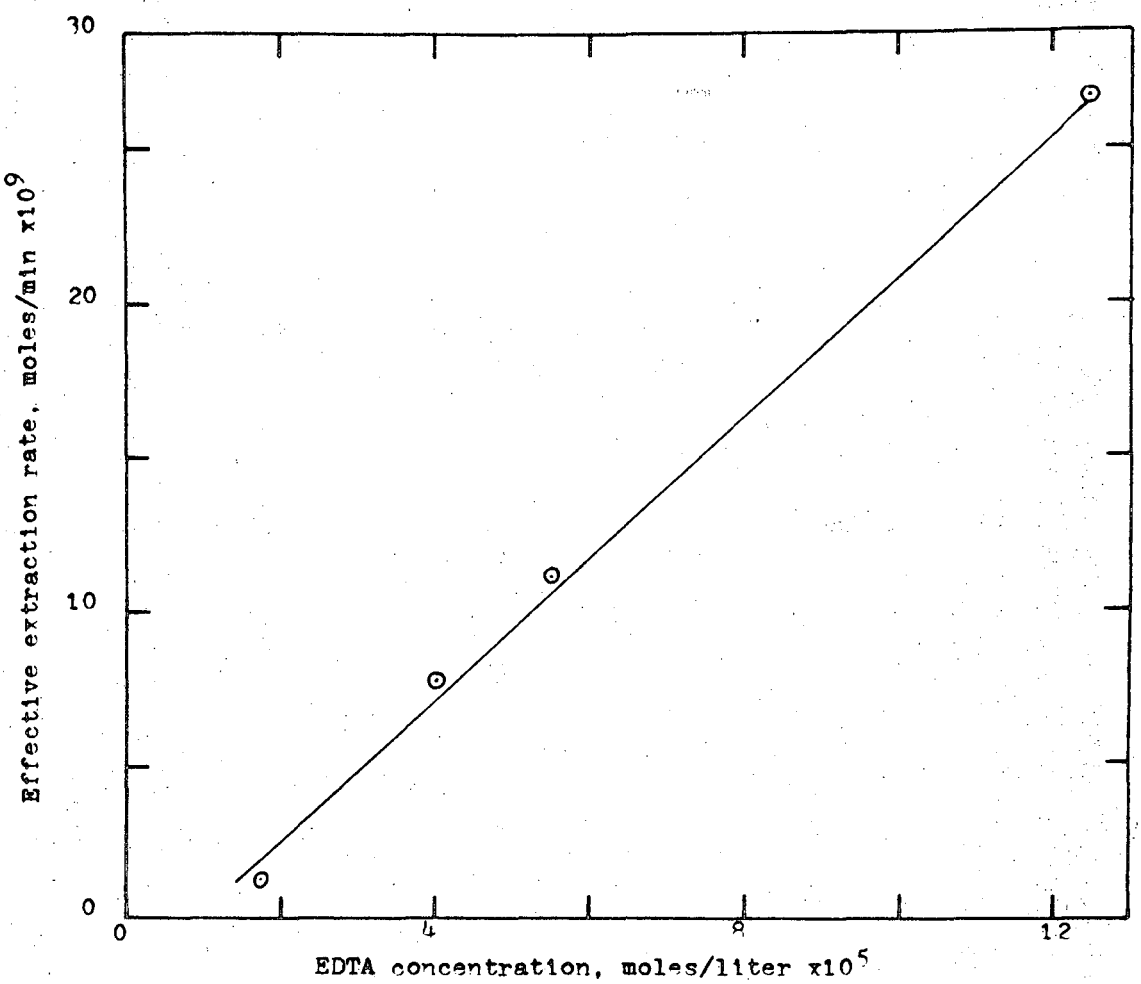

Figure 18. Effect of EDTA concentration on rare-earth extraction.

however, all of the EDTA was complexed with rare earth and the chelated rare earth was in excess of the total surfactant concentration so that the probability of occurrence of free surfactant in the solution was small. In experiment 325 and 371 no EDTA was present (hence no combined surfactant), and, again, no foam was produced even though the surfactant concentration was at a normal level. The synergistic roles of the individual constituents in foaming were not explored further; in the future, systematic measurements of bulk and surface viscosity and surface pressure might provide a more detailed understanding of the foaming process.

Separation Performance. Both the total rare-earth enrichment ratio and extraction rate (Table XV and Figure 18) increased as the EDTA concentration increased. The foam liquid rate was approximately constant, so that the observed behavior is believed to result from competition between free and combined surfactant for surface sites. For a given rare-earth and surfactant loading, higher EDTA concentrations would favor adsorption of the EDTA/rare-earth /surfactant combination.

At EDTA levels above 1.26×10^{-4} M (exp 363), precipitate was observed to form in the foam.

This EDTA concentration was taken as an approximate limiting value for rare-earth separation, because

precipitate was undesirable. Precipitate undesirability stems from complicating the handling of the foam, and because it often leads to less selective separations. The precipitation occurs because the solubility product of the surfactant/EDTA/rare-earth combination is locally exceeded as a result of surface coalescence. Foam fractionation at higher EDTA bulk concentrations might be feasible at still higher surfactant concentrations, which in principle could lower the surface concentration of combined surfactant by increased adsorption of the free surfactant.

The variation of the separation factor for foaming at different concentrations of EDTA is reported in Table XV. Semi-theoretical separation factors α_t are given for comparison, calculated from the experimental enrichments and the theoretical ratios of chelated Nd to Ce. The experimental separation factors are significantly lower; the difference may be attributable to nonspecific triple-layer adsorption of Nd and Ce as discussed earlier.

The markedly low α of 1.30 in Exp. 355, in spite of the large theoretical surface ratio of 4.10, is evidently caused by low surface adsorption at the low EDTA concentration (0.174×10^{-4} M) employed.

The results indicate that the best EDTA concentration does not lie in the low range which yields the largest surface ratio of Nd to Ce, but rather at an intermediate

concentration which gives significantly greater enrichment and thus gives a maximum separation. For the conditions of these experiments, the best EDTA concentration lies at or above 0.56×10^{-4} M. Further EDTA concentration increments into the range of precipitation are not desirable because of reduced theoretical and experimental separation factors.

Effect of pH

Control of the acidity or alkalinity of the pool liquid was found to be very important to the separation. A pH above 7.0 must be excluded because of precipitation of rare-earth hydroxides (see Table XVII). Too low a pH is undesirable because it tends to form neutral EDTA/rare-earth chelates which appear to be unextractable.

The role of the pH was evaluated by foaming at 17cm from solutions 2.14×10^{-4} M in surfactant, 2.01×10^{-4} M in Ce^{+3}, and 1.93×10^{-4} in Nd^{+3}. Most solutions included 0.551×10^{-4} M EDTA, but two had none. The results of foaming in the pH range 4.14 to 8.07 are reported in Table XV .

Effects at High pH (6.9 and Above). Precipitation of the white, gelatinous rare-earth hydroxides was obsesved at and above pH 6.90. Data of Table XVI appear to be based on instantaneous visible precipitation, rather than on aged samples and thus could be expected to be slightly higher.

Foaming from solutions at pH greater than 6.9 and containing surfactant but no EDTA was taken as evidence of

Table XV. Effect of pH on separation factor.*

run no.	pH start	pH end	feed EDTA ($Mx10^{4}$)	enrichment, E	separation factor, α	foam liquid rate (cm^3/min) $x10^2$
376	4.10	4.14	0.551	1.53±12%	1.26±15%	1.07
375	5.00	5.33	0.551	1.72±17%	2.02±17%	1.09
338	6.60	6.47	0.551	1.54±12%	----	1.36
345	6.71	6.75	0.551	2.96± 2%	1.89± 8%	1.45
377	7.92	7.95	0.551	0.98± 4%	2.60± 8%	3.81
361	6.90	6.24	none	0.85± 7%	0.92±15%	1.31
378	8.07	6.41	none	0.53±12%	----	1.42

* Hyamine $2.14x10^{-4}$ M
$NdCl_3$ $1.91x10^{-4}$ M
$CeCl_3$ $2.02x10^{-4}$ M
gas rate 0.86cm/min
height 17cm

UCRL-19525

Table XVI. The pH for incidence of precipitation of rare-earth hydroxides.

element	pH
La	8.03
Ce	7.41
Pr	7.05
Nd	7.02
	7.40
Sm	6.83
Y	6.78

Reference: T. Moeller, H.E.Kremers, Chem.Revs., 37,7(1945).

synergism between free surfactant and the hydrolyzed surfactant. The surfactant amine (M4) assumes the same stability promoting role at high pH that the combined surfactant assumes at low pH.

Unhydrolyzed surfactant may also have been present. The pH changes from 6.9 to 6.2 and from 8.1 to 6.4 (Exp. 361 and 378) for foaming in the absence of EDTA and from 7.92 to 6.95 for foaming in the presence of EDTA (Exp. 377), were taken as evidence of hydroxide extraction by the unhydrolyzed and charged surfactant.

Supporting evidence for the similarity of the surfactant amine to the combined surfactant in synergizing the foaming is seen in the similarity of liquid contents between the foams formed at low pH with EDTA present ($1.40 \times 10^{-2} cm^3$/min) and those formed at high pH without EDTA ($1.38 \times 10^{-2} cm^3$/min).

The separation performance in the pH range above 6.90 was useful to a more complete understanding of the complex phenomena occurring in this system. When no EDTA was present (Exp. 361 and 378) enrichments less than one and separation factors of about one were observed. The low enrichments reflect the precipitation of the rare-earth hydroxides, and the lack of separation indicates the non-specific action of the surfactant in the absence of EDTA.

When EDTA is present at a pH of 7.92 an enrichment of 0.98 was obtained. The low enrichment indicates the presence of the rare-earth hydroxides since they deplete the solution of free rare-earth ions. Precipitate was noted in the foam sample of this experiment and was believed to be rare-earth hydroxide activated by adsorption of EDTA on the solid surface. The separation factor of 2.60 obtained in this experiment was larger than the separation at lower pH where higher enrichments were obtained. The large separation is explained by the absence of a triple-layer adsorption since the number of free rare-earth ions has been greatly reduced by precipitation. This result emphasizes the importance of the triple-layer adsorption and points in the direction of selecting chelating systems for optimum separation which yield a charged and uncharged species rather than two charged species.

Effects at Low pH (Below 6.9). Variation of the pH in the range of well-behaved transient foaming, reported in Table XVI, indicated a rather sharp increase in enrichment from 1.54 to 2.96 at a pH between 6.47 and 6.75. Below a pH of about 6.6, the enrichment of rare earth was approximately constant at 1.54. The sharp increase in E is perhaps connected with the ionization of the EDTA/rare-earth chelate; above pH of about 6.6 all the EDTA chelate is univalent and below 6.6 significant amounts of the chelate may be neutralized by H^+. Below pH 6.6 the surfactant must compete with H^+ to achieve the observed enrichments.

Most of the experiments previously reported were for solution pH's in the neighborhood of 6.70. Collectively, they confirm the conclusion that separation is better at 6.70 than at low pH's. Because interaction between surface and bulk liquid may appreciably change the pH of the latter, it does not appear feasible to try to control pH more closely than about 0.1 of a pH unit.

The observed enrichment increase near pH 6.7 may result from hydroxide-ion initiated surface condensation. Sensitivity to pH has been reported in Langmuir-balance surface-pressure studies of interactions between metal ions and anionic surfactants (W11) where changes from an expanded (or dilute) to a condensed (or concentrated) surface layer typically occurred over a narrow pH range (0.5 to 1.0 pH units) near the pH of metal hydroxide precipitation. The activation of beryl to flotation by long-chain heavy-metal sulfonates also shows maximum extraction just below the pH of precipitation of the heavy metal hydroxide (F1). This action appears to result from a OH^- activated condensation of adsorbed collector on the solid surface of the mineral.

The mechanism by which the OH^- ion promotes condensation has been hypothesized as formation of monohydrates of the heavy metals (F1,W11) and subsequent hydrogen bonding within the surface. Hydroxide initiated condensation in the Hyamine/rare earth/EDTA system may result from (a) the

formation of monohydrates of rare earth in the coadsorbed triple layer, (b) the adsorption of OH^- into the surface by Hyamine and subsequent hydrogen bonding between OH^- and rare-earth/EDTA complexes, and (c) the hydrolysis of the surfactant to an amine and subsequent reduction of the charge repulsion between the surface species.

Effect of Induced Reflux

The class IV foaming of the preceding sections did not show improved separation with height, because the coalescing bubbles appear not to have released surface material to the intersticial liquid. This conservative action may have resulted from the rather gentle nature of the coalescence. If this is so, internal reflux may be induced by subjecting foam bubbles to strenuous distortion, so that the surface material is thoroughly mixed with the intersticial liquid, and then readsorbed with a new distribution of ions.

To test this idea, several kinds of obstructing devices were placed in the path of the upflowing foam. These devices included stainless-steel screening, plastic screening, a perforated Mylar disk, and a packed section of plastic beads. In every instance, for practical reasons, the devices were inserted at the joints between sections of the glass column. Thus, in a 24cm foam the device was at 20cm, in an 18cm foam the device was at 13cm, and in a 10cm foam the device was at 5cm.

Even the highest placement of a device (20cm) should be effective in inducing multiple contacting, since the ratio of uncomplexed to complexed rare-earth ions at 20 cm was 1:2, assuming the interstitial liquid had the pool concentration. However, in the taller columns, the fraction of ions which are not ommplexed decreases rapidly (1:3 at 25cm, for example), so that the opportunity for internal reflux to bring about a redistribution of ions is markedly smaller.

In foaming runs the feed solutions were 0.100 gm/l in Hyamine 1622, 0.536×10^{-4} M in EDTA, 1.90×10^{-4} M in Sm^{+3} or Nd^{+3}, and 2.02×10^{-4} M om Ce^{+3}; a gas rate of 0.86 $cm^3/cm^2 min$ was used. The effect of the devices on the foam liquid content, extraction rate, and separation of rare-earth ions was measured and compared to unobstructed foaming, with the results given in Table XVII .

Effect on Liquid Content. The most general observation, concerning all of the devices placed in an 18cm or shorter foam, was that their presence resulted in a higher foam-liquid volume. The magnitude of this effect was greatest in 18cm foams where 100% increases in liquid content were typical.

The increased liquid content was viewed as resulting from the action of the devices in retaining liquid and preventing drainage. As more of this liquid, which would ordinarily drain to the pool, was retained at the device, more was

Table XVII. Effect of reflux inducers on separation performance.**

run no.	inducing device	height of device in foam (cm)	total foam height (cm)	enrichment, E	separation factor, α	semi-theoretical separation factor, α_t	foam liquid rate (cm^3/min) x10^2
345	none	---	17.5	2.69± 2%	1.89± 8%	2.68	1.45
350	perforated plate	13.0	18.0	1.74± 2%	1.48± 6%	2.09	3.01
349B	perforated plate & 6cm of 9mm plastic beads	12.5	17.5	1.81± 2%	2.19± 2%	2.13	3.34
352*	none	---	17.3	1.68± 9%	3.15±16%	---	1.62
359*	30-mesh stainless steel screen	13.0	18.0	1.47± 8%	2.35±13%	---	2.42
360*	three-tier stack 30-mesh screens	13.0	18.0	0.95± 5%	4.81±12%	---	2.34
367*	two perforated plates	5.0 &13.0	18.0	1.08± 2%	1.47± 5%	---	8.23

(table continued on next page)

run no.	inducing device	height of device in foam (cm)	total foam height (cm)	enrichment, E	separation factor, α	semi-theoretical separation factor, α_t	foam liquid rate (cm^3/min) $x10^2$
336	none	---	10.0	1.06± 1%	1.09± 6%	---	11.03
349A	perforated plate	4.5	10.0	1.11± 1%	1.12± 6%	---	15.5
353*	none	---	24.5	3.82± 6%	5.61±16%	---	0.667
356*	perforated plate	20.0	24.5	2.75± 7%	---	---	0.389
369*	perforated plate	20.0	24.5	2.14± 5%	2.06±15%	---	0.628

* Indicates Sm/Ce separation; all others Nd/Ce separations.

** $CeCl_3$ $2.01x10^{-4}$M
$NdCl_3$ $1.93x10^{-4}$M
$SmCl_3$ $1.90x10^{-4}$M
EDTA $0.538x10^{-4}$M
Hyamine $2.14x10^{-4}$M

pH = 6.7
gas rate = 0.87cm/min.

carried away by the rising foam, and a steady-state foaming was reached which was wetter than the unobstructed foaming.

An extreme example of liquid retention was observed in experiment 367, where a 2 to 3mm depth of liquid accumulated on the lower of two perforated Mylar plates in an 18cm foam. The liquid content of this foam at exit was larger than that of the unobstructed foam by a factor of 5.

An exception to the general observation of increased wetness was observed in 24cm foams with a perforated Mylar plate at the 20cm level. In this case, the average liquid content (Exp. 356 and 369) of $0.507 \times 10^{-2} cm^3/min$ was about 1/3 less than the liquid content of $0.667 \times 10^{-2} cm^3/min$ for the unobstructed foam (Exp. 353). Presumably, this was a result of loss of foam because of extreme coalescence caused by the encounter of the device with the relatively dry and fragile 20cm foam.

Effect on Separation Factor. A direct improvement in the Sm/Ce separation factor from 3.15 to 4.81 was observed for the use of a three-layer stack of stainless-steel screens (Exp. 360, Table XVIII). This improvement occurred in spite of the nearly 50% increase in liquid content of this foam. In contrast to this, no improvement was obtained for foaming through a single screen (Exp. 359).

The Nd/Ce separation may have been improved by the use of a packing of glass beads. The improvement in the separation factor from 1.89 to 2.19 is viewed as significant, when

the separation factors are compared to the theoretical separation factors based on the experimental enrichment and the theoretical ratio of chelated Nd to Ce. In the case of unobstructed foaming or of a perforated plate blockage, the actual separation factor was less than the theoretical by 50%. For foaming through the plastic-bead packing, the actual α differed from the theoretical α_t by only a few percent, and constituted a significant improvement.

The effect on separation in 10cm foams was insignificant due to excessive liquid content of the foams at this height.

Effect of Material of Construction of Device. The choice of the material of construction of the device was important to the kind of action observed in the foaming. An experiment using an 18-mesh plastic screen (at 12.5cm in an 18cm foam) produced a foam so fragile that it could not pass through the foam exit section. Whenever the top layer of the foam reached the constriction at the foam-exit section, the entire mass of foam above the screen immediately collapsed back to the screen. Normal, unobstructed foaming was reestablished when the screen was removed. A waxy yellow water-soluble residue was deposited on the screen, either directly from contact with the foam or indirectly from the total coalescence of the foam above.

Although this action was not suitable for a foam fractionation in the kind of equipment used in this program, it

may have application as a collection scheme in which a plastic screen belt continuously passes across a foaming column, collects the product of total coalescence, is washed to remove the product, dried, and returns to the same or another column.

In another experiment employing an 80-mesh stainless-steel screen, no foam could pass the obstruction due to total coalescence at the screen surface.

The use of obstructing devices appears to cause separation improvement only when the device causes strenuous distortion of the foam. The presence of single screens or of a perforated Mylar plate increased the total liquid content to the foam but not the separation factor.

The results of this section indicate that a wide variety of packing configurations and materials ought to be investigated. Of particular interest would be thicker stacks or packings and packings placed at intervals in taller columns. The total coalescence of persistent foams by plastic screens might be of interest both from the standpoint of foam reduction and separation improvement.

CONCLUSIONS

Prior Art

1. The existing literature provides design guidelines for "persistent" foaming, i.e foaming which maintains bubble area (and also liquid content) invariant with height. Foam density may be predicted, but only for invariant liquid content. Surface adsorption may be predicted, for foams whose surfaces are in equilibrium with the underlying liquid.

2. Two regimes of persistent foaming are correlated in the literature: the polyhedral-bubble regime, where foam liquid fraction f is proportional to the 0.75 power of gas flowrate v_s, and the spherical-bubble regime, where f is proportional to v_s squared.

3. Selectivity in foam extraction of nonsurfactive ion species depends largely on ion-surfactant charge-interaction and complex formation, as developed by Jorné. Jorné's theory of charge interaction predicts an average separation factor of 1.05 between adjacent rare earths.

4. Rare-earth separations by precipitation have been quite difficult, and those by multistep crystallization exceedingly tedious. Among methods not involving solid formation, ion exchange separation, with complexing, has been effective in transient (chromatographic) conditions but has not been adapted to continuous operation. Liquid-liquid extraction

often requires heavy loading of an aqueous solution with auxiliary salts or acids, and also involves reextraction and attendant handling of an organic phase.

5. Foam fractionation has been applied to rare-earth processing for separation from other metals (Sr^{+2}, Cs^{+}, Sc^{+3}), but not to separations between the lanthanides.

New Developments in the Present Study

1. The model of "persistent" foaming does not apply to most of the foaming conditions which were found in this study to favor foam formation, extraction, and fractionation. A two-property classification was therefore adopted, the type being determined by the persistence or transience of surface area, and the mode by the constancy or depletion of specific liquid content with foam height or age. The consequence of a successful demonstration of foam fractionation in the transient regime of foaming is that many weakly foaming substances hitherto rejected for the purpose can in fact be used advantageously.

2. Solutions of an anionic surfactant (Aerosol-22) exhibited transient foaming at low, and persistent foaming at high, gas rates. In the transient regime, f was proportional to the 0.2 power of v_s. Maximum enrichment was observed for the most transient foaming. Maximum extraction occurred at somewhat higher gas rates, (still within the range of transient foaming) which increased as the solution concentration

decreased. High foam-liquid rates such as are encountered in persistent foaming appear quite unfavorable for extraction because they represent a large entrainment of bulk liquid.

3. As with ion exchange or extraction, chelation or similar complexing appears essential for providing reasonable separations between rare earths in foam fractionation. Although a surfactant which also enters into selective complex formation might be found, these two functions were served in the present experimental program by a cationic surfactant (Hyamine 1622) and by EDTA. To obtain foaming, both free surfactant and surfactant-EDTA-metal (or hydroxide) complex were required. Foaming of this system shows transient surface-area behavior and diminishing liquid content per unit area; transiency increases as surfactant concentration decreases.

4. Rare-earth enrichments increased continuously with height in the foam. Effective extraction rates were constant at foam heights above 17cm. Constancy of extraction, in spite of surface loss, was viewed as a conservation of total rare-earth mass on the diminishing surfaces. Separation factors (α) for the Nd/Ce separation were 1.9, and for Sm/Ce 3.85 above 17cm. The separation factor drops sharply toward 1.0 at shorter heights. Evidence of non-specific coadsorption of rare earth was observed, since the value of α expected on the basis of the liquid-phase equilibrium was not reached.

5. The lowest surfactant concentration (0.03g/l) that will still produce foaming (of the most transient type), also yields the best separation factor and enrichment at constant height.

6. Extraction rates increase proportionately to increasing EDTA concentration at fixed rare-earth and surfactant levels, but are accompanied by decreasing selectivity.

7. At a relatively high EDTA solution concentration (1.3×10^{-4} M), a light precipitate (presumably containing EDTA, rare earth, and surfactant) forms. This condition is operationally undesirable, and also departs from pure foam fractionation, therefore setting an upper limit to the allowable EDTA level which appears to be relatively insensitive to the variations allowable in rare-earth and surfactant levels.

8. A pool-liquid pH above 6.9 causes bulk precipitation of rare-earth hydroxides. Maximum separation and extraction are obtained adjacent to this limit. Hence a pH near 6.7 is recommended as optimum.

9. Reflux inducement by inserting obstructions was effective in improving the separation factor in cases of prolonged distortion of the foam matrix. For plastic bead packings or stacked three-tier stainless-steel screens, the α for Nd/Ce was raised from 1.9 to 2.2, and the α for Sm/Ce from 3.1 to 4.8. Single screens and single finely perforated

plates were found to reduce drainage and increase the foam liquid-content, but without altering the α. Still other materials (plastic screens; small-mesh stainless-steel screens) rejected liquid more completely and hence destroyed the foam.

Suggestions for Future Work

1. By contrast to the present study which focusses upon extraction of complexed rare earth, it appears that higher α values will probable be obtained by using an anionic surfactant which will interact with and co-adsorb only unchelated rare-earth cations. Also, the low surface area typical of many anionic surfactants may provide higher molar concentrations per unit surface area, and thus lead to greater enrichments.

2. Because of its potential as the basis of more and better foam-fractionation processes, transient foaming should be investigated thoroughly. For example, further study of liquid-content variation with gas rate is needed. Because of the lower strength of a foam column in transient foaming, stabilizing vanes or guide-wires may be needed in large-diameter columns.

3. Reflux-inducing devices deserve much broader study with respect to their surface properties, degree of deformation of the foam, and duration of contact. For instance, long sections of a suitable packing followed alternatively by drainage sections might prove to be very effective in

promoting multiple contacts. Application of such devices in persistent foaming systems might produce stepwise drops in liquid content with attendant improvement in the separation performance.

Overall Prospects

1. The overall prospects for foam fractionation are directly related to the features listed below:

   a. It operates in a low concentration range.
   b. High degrees of purification are possible.
   c. Product recovery is easy.
   d. Supplementary processing to recover surfactant from the concentrated foam liquid is accessible.
   e. The process consumes a minimum of materials and produces little waste.
   f. It is operationally very simple.
   g. Power requirements are low because of very low pressure drops through the equipment.

2. Although the method is studied here only for metal salts, it may be well suited for separating and recovering many other compounds including organic contaminants in water supplies.

3. Application may be made to processing and recovery of actinides and fission products if suitable chelating species are employed.

NOTATION

a_i = activity of species i (moles/l)

A = ratio of surface area to foam liquid volume

Å = Angstroms (10^{-8}cm)

c_j = concentration, j = s, p, f (moles/l)

c_{ij} = concentration, i = components a,b,c,...
j = flowstreams s,p,f (moles/l)

d = diameter of individual bubbles (mm)

$\bar{d}^2$ = squared average diameter $= \sum_i n_i d_i^3 / \sum_i n_i d_i^2$ (mm)

D = dimensionless dielectric constant

D_o = 1.112×10^{-12} coul/volt·cm

D_c = foaming column diameter (cm)

D_{32}^2 = $\bar{d}^2$

e = electronic charge = 1.602×10^{-19} coul.

E = enrichment ratio

f = volume fraction of liquid in foam

F = volumetric feed rate (cm^3/min)

G = volumetric gas rate (cm^3/min)

k = Boltzmann constant = 1.38×10^{-16} erg/molecule·°K

k_i = empirical constant, i= 1,2,3,4....

K_I = formation constants for complexes with metal ions and complexing agents, I = A,B....

m = empirical constant

M = effective extraction rate (moles/min)

$\underline{M}$ = moles/l

$n_{\infty i}$ = bulk number concentration of i (number/cm^3)

N = molecular weight (g/mole)

P = pool volumetric withdrawal rate (cm^3/min)

q = specific liquid content (cm)

R = reflux ratio of liquid returned to column/ liquid recovered as product

S = surface generation rate (cm^2/min)

S_b = volumetric rate of liquid in foam not associated with the surface (cm^3/min)

S_v = volumetric rate of total foam liquid (cm^3/min)

t = time (min)

T = absolute temperature (^oK)

v_s = gas velocity (cm/sec)

v = $\exp(-e\Psi/kT)$

v_o = v at $x = x_o$

x = distance from interface into the intersticial liquid

z_i = charge of species i

z_s = charge of surfactant ion

Subscripts:

c = surfactant

f = feed

p = pool

s = foam

Greek letters:

α = separation factor

β = relative distribution factor

ϵ = foam density (gm/cm^3)

γ = surface tension (dynes?cm)

Γ = surface adsorption density of species i ($moles/cm^2$)

Ψ = electrical potential (erg/coul)

π = 3.1416

ρ = liquid density (g/cm^3)

ρ_c = net charge density ($coul/cm^3$)

μ = chemical potential of species i

μ = liquid viscosity (centipoise)

ACKNOWLEDGMENT

The research was performed under the auspices of the U.S. Atomic Energy Commission. The first named author acknowledges with thanks a Standard Oil Company of California Research Fellowship.

The gift of Aerosol-22 and Hyamine 1622 from American Cyanamid and Rohm and Haas is acknowledged. The authors thank the Lawrence Radiation Laboratory glass shops for their assistance in constructing the apparatus.

Figures 1 and 2 were adapted from the paper by Lemlich (L2).

The suggestions and comments of Professor D.W. Fuerstenau are gratefully acknowledged.

REFERENCES

A1 A.W. Adamson, Physical Chemistry of Surfaces, 2nd ed. (Interscience, New York, 1967), p.234.

A2 Anonymous, C.&E.N., 78, (May10,1965).

B1 D.J. Bauer, USBM-5942, 1962.

B2 K.J. Bril in Progress in the Science and Technology of Rare Earths, Vol. 1 (Pergamon Press, New York, 1964), p.30,47.

B3 C.A. Brunner, R. Lemlich, I.&E.C. Fund. 2, 297 (1963).

B4 J.J. Bikerman, Foams: Theory and Industrial Application (Rheinhold Publishing Co., New York, 1953).

C1 F.A. Cotton, G. Wilkinson, Advanced Inorganic Chemistry (Interscience, New York, 1962), p.870.

C2 K.L. Cheng, R.H. Bray, Anal. Chem. 27, 782 (1955).

D1 J.T. Davies, E.K. Rideal, Interfacial Phenomena, 2nd ed. (Academic Press, Inc., New York, 1963), p.186,234.

D2 F.P. Dwyer, D.P. Mellor, Chelating Agents and Metal Chelates (Academic Press, New York, 1964).

E1 I.A. Eldib in Advances in Petroleum Chemistry and Refining, Vol.7 (Interscience, New York, 1963), Chp.2.

E2 R.C. Evans, An Introduction to Crystal Chemistry (Cambridge University Press, Cambridge, 1966).

F1 M.C. Fuerstenau, P. Somasundaran, D.W. Fuerstenau, D.A. Rice, Trans. Inst. Min.&Met. 74, part 7, 381 (1964-5)

G1 E.D. Goddard, O. Kao, H.D. Kung, J.Coll.&Int.Sci. 27, 616 (1968).

G2 R.B. Grieves, D. Bhattacharyya, W.L. Conger, Chem.Eng. Prog.Sym.Ser. 65, No. 91,29 (1969).

G3 R.B. Grieves, S. Kelman, W.R. Obermann, R.K. Wood, Can. J.Chem.Eng. 41, 252 (1963).

G4 R.B. Grieves, T.E. Wilson, Nature 205, 1066 (1965).

H1 P.A. Haas, H.F. Johnson, A.I.Ch.E.J. 11, 319 (1965).

H2 P.A. Haas, H.F. Johnson, I.&E.C.Fund. 6, 235 (1967).

H3 E.C. Hunt, J.Coll.&Int.Sci. 29, 105 (1964).

J1 C. Jacobelli-Turi, S. Terenzi, A. Barocas, I.&E.C.Proc. Des.&Dev. 6, 161 (1967).

J2 C. Jacobelli-Turi, S. Terenzi, M. Palmera, I.&E.C.Proc. Des.&Dev. 6, 162 (1967).

J3 J. Jorne, Unpublished PhD qualifying examination, University of California, Berkeley (Spring 1968).

J4 J. Jorne, E. Rubin, I.&E.C.Fund. 8, 474 (1969).

K1 B.L. Karger, R.B. Grieves, et.al., Sepm. Sci. 2, 401 (1967).

K2 I. Koizumi, Kagyo Kagaku Zasshi 70, 1641 (1967) or Chem.Abs. 69, 56765 (1968).

K3 H.E. Kremers in Encyclopedia of Chemical Technology, Vol.11 edited by R.E.Kirk and D.F. Othmer (Interscience, New York, 1953), p.503.

K4 J.A. Kitchener in Recent Progress in Surface Science, Vol.1 (Academic Press, New York, 1964),p.51.

K5 J.A. Kitchener, C.F. Cooper, Chem. Soc.London Quart. Rev. 13, 71 (1959).

L1 R. Lemlich, Chem.Eng. 75, no. 27, 95 (1968).

L2 R. Lemlich, I.&E.C. 60, 16 (1968).

L3 R. Lemlich in Progress in Separation and Purification, Vol.1, edited by E.S. Perry (Interscience, New York, 1968), Chp.1.

L4 R.A. Leonard, R. Lemlich, A.I.CH.E.J. 11, 18 (1965).

L5 Ibid. 11, 25 (1965).

L6 H.A. Laitinen, Chemical Analysis (McGraw Hill, New York, 1960), p.229.

M1 A.E. Martell, M. Calvin, Chemistry of the Metal Chelate Compounds (Prentice Hall, New Jersey, 1956).

M2 T. Moeller, H.E. Kremers, Chem. Revs. 37, 917 (1945).

M3 E.A. Moelwyn-Hughes, Physical Chemistry, 2nd ed., (Pergamon Press, New York, 1961).

M4 J.L. Moilliet, B.Collie, W. Black, Surface Activity, 2nd ed., (D. Van Nostrand Co., New Jersey, 1961).

M5 Molybdenum Corporation of America (New York) private communication, 1968.

M6 J.K. Marsh, J.Chem. Soc. Part I, 451 (1955).

P1 J.G Parker in Minerals Yearbook edited by K.L. Wang and E.E. Johnson (U.S.B.M., Washington,D.C., 1964) p.893.

P3 J.E. Powell in Progress in the Science and Technology of Rare Earths, Vol.1,(Pergamon Press, New York, 1964) P.62.

P4 J.E. Powell, F.H. Spedding Chem. Eng. Prog. Sym. Ser., no. 24, 55, 101 (1959).

P5 D.F. Peppard in The Rare Earths edited by F.H. Spedding and A.H. Daane (John Wiley and Sons, Inc., New York, 1961),Chp.4.

R1 A.J. Rubin, J.A.W.W.A. 60, 834 (1968).

R2 E. Rubin, R. Everett, I.&E.C. 55, 45 (1963).

R3 E. Rubin, E.L. Gaden in New Chemical Engineering Separation Techniques (Interscience, New York, 1962), Chp.5.

R4 A.J. Rubin, J.D. Johnson, J. Lamb, I.&E.C.Proc.Des.&Dev. 5, 368 (1966).

R5 E. Rubin, C.R. LaMantia,E.L. Gaden, C.E.S. 22, 1117 (1967).

R6 E. Rubin, M.S. Hoffer, I.&E.C.Fund. 8, 483 (1969).

R7 Rohm and Haas Co., Technical Bulletin SAN 1-6, September, 1968.

S1 R.W. Schnepf, E.L. Gaden, E.Y. Mirocznik, E. Schonfeld, C.E.P. 55, 42 (1950).

S2 H.M. Schoen, Ann. N.Y.Acad.Sci. 137, 148 (1966).

S3 H.M. Schoen, P.M. Krishna, Radium Removal from Uranium Mill Waste Streams, USPHS-7409-c1, June 15, 1962.

S4 H.M. Schoen, G. Mazella, Ind. Water & Wastes 6, 71 (1961).

S5 E. Schonfeld, R.Sanford, G. Mazella, D.Ghosh, S. Mook, USAEC NYO-9577, 1960.

S6 F. Sebba, Ion Flotation (Elsevier Pub. Co., New York, 1962).

S7 F. Sebba, Nature 184, 1062 (1959).

S8 F. Sebba, J.A. Lusher, J.Appl.Chem. 15, 577 (1965).

S9 F. Sebba, N.W. Rice, J.Appl.Chem. 15, 105 (1965).

S10 W.L. Silvernail, R.M. Healy in Encyclopedia of Chemical Technology 2nd ed., Vol.4., edited by R.E. Kirk and D.F. Othmer (Interscience, New York, 1963), p. .

S11 S.P. Sinha, Complexes of the Rare Earths (Pergamon Press, New York, 1966).

S12 M.E. Stephenson, Application of Foam Fractionation to Sewage Treatment USPHS WP-00396, September 1964.

S13 G. Schwarzenbach, Complexometric Titrations (Interscience, New York, 1957), p.73,74.

S14 F. Sebba, M.W. Rose, J.Appl.Chem. 19, 185 (1969).

S15 F. Schutz, Trans. Far.Soc. 41, 437 (1946).

T1 E.R. Tompkins, S.M. Mayer, J.Amer.Chem. Soc. 69, 2859, (1947).

V1 R.C. Vickery, Analytical Chemistry of the Rare Earths (Pergamon Press, New York, 1961), p.20.

W1 P.F. Wace, P.J. Alder, D.L. Banfield, Chem.Eng.Prog. Sym. Ser. 65, No.91, 19 (1969).

W2 P.F. Wace, D.L. Banfield, Chem.&Proc.Eng. 47,71 (1966).

W3 P.F. Wace, D.L. Banfield, Nature 206, 1131 (1965).

W4 C. Walling, E.E. Ruff, J.L. Thornton, J.Phys.Chem. 61, 486 (1957).

W5 B.Weaver, Anal. Chem. 26, 474 (1954).

W6 B. Weaver in Progress in the Science and Technology of the Rare Earths, Vol.1 (Pergamon Press, New York, 1964), p.85.

W7 C.L. Wilson, D.W. Wilson, Comprehensive Analytical Chemistry, Vol.1C (Elsevier, New York, 1962), p.485.

W8 Ibid. pp. 449-451.

W9 Ibid. pp.453-454.

W10 C.L. Wilson, D.W. Wilson, Comprehensive Analytical Chemistry, Vol.1B (Elsevier, New York, 1960), Chp.VII-9, Chp.VIII-3c.

W11 G.A. Wolstenholme, J.H. Schulman, Trans.Far.Soc. 46, 475 (1950), and 47, 788 (1951).

TECHNICAL INFORMATION DIVISION
LAWRENCE RADIATION LABORATORY
UNIVERSITY OF CALIFORNIA
BERKELEY, CALIFORNIA 94720